



<PE-AT>MORE THAN ONE WAY TO BE A GIANT: CONVERGENCE AND DISPARITY IN THE HIP JOINTS OF SAURISCHIAN DINOSAURS

Henry P. Tsai¹, Kevin M. Middleton², John R. Hutchinson³, Casey M. Holliday²

¹ Department of Biomedical Sciences, Missouri State University, Springfield, Missouri, 65897. U. S. A.

² Department of Pathology and Anatomical Sciences, University of Missouri, Columbia, Missouri, 65212. U.S.A.

³ Structure & Motion Lab, The Royal Veterinary College, North Mymms, Hertfordshire, United Kingdom.

Running title: Saurischian hip joint and body size evolution

Corresponding author: Henry P. Tsai., Contact information: HTsai@missouristate.edu

Author contributions: HPT conceived the study. KMM, CMH and HPT designed the study. HPT, KMM, and CMH analysed data with additional support and discussion by JRH. HPT drafted the manuscript, with critical evaluation and approval for submission by KMM, JRH, and CMH.

Acknowledgments: This study greatly benefited from discussions with A. Hammond, K. Sellers, S. Werning, R. Menegaz, T. Owerkowicz, A. Summers, and H. Mallison. The authors are grateful to S. Nesbitt for providing a research quality cast of *Asilisaurus kongwe*; to H. Mallison for providing CT-scan data of *Plateosaurus*; and to W. Parker for providing laser scan data for *Coelophysis* for this study. We would like to thank all of the curators and staff for access to fossil specimens and permission for digital data collection. We thank C.

This article has been accepted for publication and undergone full peer review but has not been through the copyediting, typesetting, pagination and proofreading process, which may lead to differences between this version and the [Version of Record](#). Please cite this article as [doi: 10.1111/evo.14017](#).

This article is protected by copyright. All rights reserved.

Ward and L. Cowgill for reviewing early drafts of this manuscript, which was part of HPT's University of Missouri doctoral dissertation. We would also like to thank three anonymous reviewers for providing helpful critiques in improving the manuscript. HPT was supported by Jurassic Foundation Research Grant, the Doris O. and Samuel P. Welles Research Fund, the University of Missouri Life Science Travel Grant, as well as Brown University's Bushnell Research and Education Fund. JRH was supported by Natural Environment Research Council grants NE/G005877/1 and NE/K004751/1. CMH was supported by the University of Missouri Department of Pathology and Anatomical Sciences, the Missouri Research Board, and the University of Missouri Research Council.

Conflict of Interest Statement: The author declare no conflicts of interest in preparing this article.

Data Accessibility Statement: The phylogenetic trees and character matrices used in this study are available as Supplementary Information of the enclosed manuscript, and are electronically archived on Dryad (doi:10.5061/dryad.hmgqnk9dc). 3D morphometric data (including surface models and raw CT scan data) are digitally archived as part of the Comparative Anatomy Inventory at Missouri State University.

ABSTRACT

Saurischian dinosaurs evolved seven orders of magnitude in body mass, as well as a wide diversity of hip joint morphology and locomotor postures. The very largest saurischians possess incongruent bony hip joints, suggesting that large volumes of soft tissues mediated hip articulation. To understand the evolutionary trends and functional relationships between body size and hip anatomy of saurischians, we tested the relationships among discrete and continuous morphological characters using phylogenetically corrected regression. Giant theropods and sauropods convergently evolved highly cartilaginous hip joints by reducing supraacetabular ossifications, a condition unlike that in early dinosauromorphs. However, transitions in femoral and acetabular soft tissues indicate that large sauropods and theropods built their hip joints in fundamentally different ways. In sauropods, the femoral head possesses irregularly rugose subchondral surfaces for thick hyaline cartilage. Hip articulation was achieved primarily using the highly cartilaginous femoral head and the supraacetabular labrum on the acetabular ceiling. In contrast, theropods covered their femoral head and neck with thinner hyaline cartilage and maintained extensive articulation between the fibrocartilaginous femoral neck and the antitrochanter. These findings suggest that the hip joints of giant sauropods were built to sustain large compressive loads whereas those of giant theropods experienced compression and shear forces.

<PE-FRONTEND>

INTRODUCTION

Saurischian dinosaurs, which include birds, non-avian theropods, sauropodomorphs, and stem taxa, range in body size over seven orders of magnitude (Benson et al., 2014) and underwent multiple, independent evolutionary transitions towards both gigantism (Sander et al., 2004; Lee et al., 2014b) and miniaturization (Stein, et al., 2010; Turner et al., 2007).

Moreover, saurischians evolved a great diversity of limb bone morphologies, suggesting an equally diverse range of locomotor behaviors (Carrano 2001; Hutchinson 2006). Therefore, saurischians are an invaluable clade for exploring the evolutionary relationships between appendicular anatomy and body size. However, inferences of joint loading, range of motion, and kinematics remain challenging because articular soft tissue is rarely preserved in fossils (Holliday et al., 2010; Bonnan et al., 2013; Bishop et al., 2018). In many archosaurs, the terminal, subchondral surfaces of limb bones differ in shape and size, such that substantial assumptions about soft tissues are needed to reconstruct the physical articulation of adjacent bony elements (Hutchinson et al., 2005; Gatesy et al., 2009). Moreover, many dinosaurs possess rugose subchondral surfaces, similar to the ossifying growth plates of juvenile birds, mammals, and lepidosaurs (Owen, 1841a, b; 1875; Marsh, 1896).

These lines of evidence indicate that gigantic saurischians (>2 tons) constructed their articular surfaces using enormous volumes of soft tissue (Cope, 1878; Hay, 1908; Holliday et al., 2010) to cope with increased loading. Interactions among articular soft tissues, such as epiphyseal cartilages, fibrocartilaginous pads, and joint ligaments serve to maintain load-bearing ability of appendicular joints in vertebrates (Carter et al, 1998; Carter and Beaupre, 2007). Limb joint loading is an especially critical issue for gigantic terrestrial vertebrates because whereas joint surfaces generally scale to the surface area of the organism, body mass scales to the organism's overall volume (Schmidt-Nielsen, 1984). Additionally, joint soft tissues provide constraints to the mobility of joints via correspondingly shaped articular surfaces (Carter and Wong, 2003; Hall, 2005) and allows longitudinal growth of limb bones at the growth plate prior to skeletal maturity (Haines, 1942a). These necessary functions are relevant to the construction of appendicular joints in vertebrates across the entire spectrum of

body size. Therefore, evolutionary transitions in body size are expected to exert selective pressures on appendicular joint anatomy of terrestrial vertebrates.

Substantial work has been devoted to the relationship between body size and bony appendicular joint morphology among vertebrates (e.g., mammals: Biewener, 1991; Godfrey et al., 1991; dinosaurs: Wilson and Carrano, 1999; Carrano, 2000; Hutchinson et al., 2005), but few studies thus far have tested the relationship between articular soft tissue adaptations with body size (Malda et al., 2013). Extant amniotes have highly disparate joint soft tissue morphologies, including the independent evolution of epiphyseal centers in mammals and lepidosaurs (Moodie, 1908; Haines, 1941; 1942a; 1942b; 1975; Enlow, 1969; Buffrénil et al., 2004), the inclusion of fibrocartilage in sliding joints (Barnett, 1954), and the the vascularized hyaline cartilage in turtles (Snover and Rhoudin, 2008) and some birds (Graf et al., 1993). In particular, archosaurs retain a single layer of epiphyseal cartilage for maintaining joint articulation, as well as longitudinal bone growth prior to skeletal maturity (Haines 1938, 1941). The epiphyseal cartilage of archosaurs contains both hyaline cartilage and fibrocartilage (Tsai and Holliday, 2015), although the contribution of each tissue, as well as the overall thickness of the epiphyseal cartilage, differs among different groups (birds: Cracraft, 1971; Firbas and Zweymüller, 1971; crocodylians: Fujiwara et al., 2010; Holliday et al., 2010; non-avian dinosauromorphs: Tsai et al., 2018). These derived morphologies among archosaurs complicate inferences of the ancestral condition and body size adaptations, and present major hurdles in studies of amniote locomotor evolution and joint functional biology.

Here we show that giant saurischian-line dinosaurs built their hip joints in two fundamentally different ways. Discrete characters or osteological correlates of articular soft tissues were combined with continuous characters, which included both linear and area measurements of the subchondral surfaces. Dimensional incongruences between the femoral

and acetabular subchondral surfaces were used as proxies for the amount of soft tissues once present in the hip joint. We then used phylogenetic comparative methods to test whether gigantic saurischians evolved highly cartilaginous hip joints. Our results will inform reconstructions of dinosaur joint anatomy, as well as its mechanical and physiological adaptations, and comparisons with other clades such as mammals.

MATERIALS AND METHODS

Osteological correlates and anatomical reference axes:

A generalized anatomical summary of archosaurian hip joint soft tissue articulation is provided in Fig. 1. Anatomical abbreviations are summarized in Table 1, and the osteological correlates of articular soft tissues are illustrated in Fig. 2. To characterize the suite of morphological transitions within the saurischian crown lineage, nomenclature for osteological correlates of joint ligaments follows Tsai and Holliday (2015) and evolutionary patterns detected in Tsai et al. (2018). In all extant archosaurs, an unossified inner acetabular wall is the osteological correlate for presence of an acetabular membrane. Therefore, acetabular membranes are inferred to be present in extinct saurischians that also possess unossified inner acetabular walls. Since the inner acetabular wall is not osseous in many archosaurs, the *bony acetabulum* is defined as the tube-shaped osseous surface of the acetabulum. In contrast, the socket-shaped surface formed by the perforated, tubular bony acetabulum and the membranous inner acetabular wall is termed the *acetabular fossa*. The cranial, osseous portion of the supraacetabulum consists of the acetabular labrum, the attachment of which can be distinguished by the absence of growth plate surfaces (Tsai and Holliday, 2015). The caudal portion of the supraacetabulum consists of the ischial peduncle of the ilium and the ilial peduncle of the ischium. Lateral expansions of the two peduncular growth plate surfaces

form the bony antitrochanter, which supported a cartilaginous articular surface distinct from acetabular labrum. The surface area of the bony antitrochanter is used as the proxy for the size of the cartilaginous antitrochanter (Fig. 3).

On the proximal femur, the cartilaginous cap consists of a hyaline cartilage core and a peripheral fibrocartilage sleeve. The hyaline core attaches to the calcified cartilage-covered growth plate surface and is confluent between the femoral head (capitular) and trochanteric regions. If the thin layer of calcified cartilage is weathered away, the growth plate surface can be identified by the exposed trabecular bone immediately deep to the calcified cartilage layer. Surface area of the growth plate is used as the proxy for the extent of the epiphyseal hyaline cartilage attachment. The fibrocartilage sleeve attaches to a collar of metaphyseal cortical bone surrounding the growth plate and proximally overlaps the capitular extent of the femoral head and trochanteric region of the femoral neck, forming a layered fibro-hyaline cartilage structure in these regions. The metaphyseal collar can be distinguished from growth plate surface by a prominent metaphyseal line and from the bony diaphysis by a prominent ridge. Surface area of the metaphyseal collar is used as the proxy for the extent of the fibrocartilage sleeve (Fig. 3). To account for the evolutionary shifts in femoral condylar orientation among saurischians, such as the independent evolution of a medially deflected femoral head among lineages (Carrano, 2000; theropods: Hutchinson, 2001b; sauropodomorphs: Martínez and Alcober, 2009; Yates et al., 2010), we use reference axes (Tsai and Holliday, 2015) to navigate the evolutionary changes in femoral head position and morphology (Fig. 2d).

Data collection:

A broad phylogenetic sample of sauropsids (N = 107 taxa; Table S1), including 51 theropods and 30 sauropodomorphs, was used to assess continuous and discrete osteological characters on the proximal femur and the acetabulum. For taxa represented by multiple

individuals (e.g., *Allosaurus*), we scored only consistent osteological character states on individuals inferred as adults or large subadults. The inclusion of subadults is merited because many nonavian archosaurs attain sexual maturity long before the onset of skeletal maturity (Erickson, 2005; Erickson et al., 2004; 2007; Lee and Werning, 2008), such that species may be defined based on character states exhibited by reproductively functional individuals that were nevertheless undergoing active skeletal growth (Hone et al., 2016). For taxa represented only by a single holotype individual (e.g., *Carnotaurus*) the individual is assumed to be an adult or subadult, unless it was noted as a young juvenile or neonate individual in literature. We excluded young juveniles and neonates from this analysis. Institutional abbreviations are summarized in Table S2.

Fossil specimens were studied by observation, linear measurements, and digital photography (Sony DSC-F828). Many specimens (N = 68 taxa) were reconstructed as surface models using 3D imaging techniques including computed tomography (CT), surface laser scanning, and photogrammetry (See Appendix S1). All 3D models were converted into .ply and .stl file formats and imported into Geomagic (V11) for analyses. The use of 3D models allowed quantitative assessment of continuous, three-dimensional osteological characters on the subchondral surfaces.

Discrete character coding:

The hip joints of saurischian-line archosaurs were examined for discrete characters, including osteological correlates of hip joint articular soft tissues. Hip joint articular soft tissues of diapsids and their 15 osteological correlates are detailed in Table 2. The purpose of these correlates was to aid in constructing discrete characters for analysis. We identified 14 osteological characters based on osteological correlates of homologous articular soft tissues among extant diapsids (Tsai and Holliday, 2015). These osteological characters served as

proxies for the presence, orientation, thickness, and shapes of articular soft tissues, and are illustrated in detail in our previous study (Tsai et al., 2018). Results from the ancestral state reconstruction were used to establish the ancestral versus derived states for each of the discrete characters presented here.

It is noted that in this study, we have chosen to score the character state of femoral head deflection (character 7) based on the binary scheme used in Tsai et al., 2018 (also Carrano, 2000; Hutchinson, 2001a), such that a craniomedially oriented femoral head has a proximodistal angle $\sim 45^\circ$ (or greater), whereas a medially oriented femoral head has a proximodistal angle closer to 0° (Fig. 1E in Tsai et al., 2018). We are aware that medial deflection of the femoral head should more accurately be coded as a continuous character, but chose to use a binary coding scheme in light of the tendency for postmortem deformations to alter or exaggerate the in vivo orientation of the femoral head. Additionally, we took care to exclude obviously crushed or deformed femora in our sample (based on overall condition of the bone).

Continuous dimensional measurements:

In order to maintain the broad phylogenetic scope of the current study, one representative individual was selected from each taxon for continuous character analysis. Criteria for choosing the representative individual includes an adequate quality of subchondral preservation, completeness of hip joint elements, and inferred ontogenetic status as an adult or subadult. As such, the representative individual may not necessarily be the holotype (e.g., *Tyrannosaurus*) or the largest individual described within its taxon (e.g., *Diplodocus*). Linear dimensions were measured using a SPI 31-518-4 dial caliper and a tape measure on physical specimens, as well as from reconstructed 3D surface models of hip joints using the *measure distance* function of Geomagic (V11 see Appendix S1). Surface area

dimensions were measured from reconstructed 3D surface models of hip joints by highlighting relevant osteological correlates and using the *select area* function of Geomagic (V11 see Appendix S1). Body mass estimates of fossil sauropsid vary widely depending on the methods used (e.g., Anderson et al., 1985; Gunga et al, 1999; 2007; Seebacher, 2001; Therrien and Henderson, 2007; Allen et al., 2009), particularly considering the uncertainty in soft tissue contribution to body dimensions (Hutchinson et al., 2011). Therefore, this study used femur length as an overall proxy for body size following Turner and Nesbitt (2013) and Lee et al. (2014), as femur length has been shown to be a reasonably reliable predictor for overall body size of archosaurs (Christiansen and Fariña, 2004; Farlow et al. 2005); although we acknowledge that minimal stylopodial circumference has some statistical superiority (Campione et al., 2012).

All continuous data were log-transformed prior to phylogenetic comparative analysis. Taxa for which a quantitative character was zero were excluded from the allometric analyses concerning that character. For example, the proximal femora of basal archosauromorphs *Chanerasuchus*, *Hyperodapedon*, and the phytosaur TMM 43685 lack a distinct separation between the metaphyseal collar and the subchondral growth plate; therefore these taxa were excluded from the analysis for metaphyseal collar surface area.

Phylogenetic Comparative Analysis

Phylogenetic tree construction:

We used phylogenetic comparative methods to investigate the association between body size and hip joint anatomical characters. Osteological correlates were used as proxies for articular soft tissues. Composite phylogenetic trees (Fig. 4) were constructed using Mesquite (V2.73) based on published studies, with branch lengths based on hypothesized

divergence date between sister clades and sister taxa (Archosauromorpha, Ezcurra et al., 2014; Archosauriformes, Brusatte et al., 2010a; Nesbitt, 2011; Dinosauromorpha, Langer et al., 2013; Brusatte et al., 2010b; Sauropodomorpha, Wilson, 2005; Martínez and Alcober, 2009; Theropoda, Carrano et al., 2012; Paraves, Turner et al., 2012; Xu et al., 2010; Aves, Clarke, et al., 2005; Ericson et al., 2006; Brown et al., 2008; Phillips et al., 2010). Pterosaurs were excluded from this analysis because the appendicular morphology in the earliest known taxa is already highly derived (Middleton and English, 2014). We constructed a “consensus” phylogenetic tree (Fig. 4a), in which Silesauridae is considered as non-dinosaurian Dinosauriformes (Brusatte, 2010b; Nesbitt, 2011), Herrerasauridae as basal theropods (Sues et al., 2011), *Eoraptor* as the basal-most sauropodomorph (Martínez and Alcober, 2009), and *Archaeopteryx* as the basal-most avialan (Turner et al., 2012). Additionally, we modified the consensus phylogenetic tree to account for five ambiguous phylogenetic placements of key taxa within Dinosauromorpha (Fig. 4b-f, See Appendix S1). We analyzed alternative tree topologies in which Silesauridae are considered stem-ornithischians (Langer and Ferigolo, 2013), Herrerasauridae as the basal-most saurischians (Novas et al., 2010), *Eoraptor* as a basal theropod (Sues et al., 2011), and *Archaeopteryx* as a stem-deinonychosaur (Xu et al., 2011; Godefroit et al., 2013). For both the consensus (Fig. 4a) and the four alternative tree topologies that followed (Fig. 4b-e), we followed the phylogenetic position of the major dinosaurian clades as proposed by Seeley (1887), in which Sauropodomorpha and Theropoda are included within Saurischia, and together with Ornithischia form Dinosauria. However, in light of a novel challenge to this reconstruction by Baron et al., (2017), we applied a more drastic modification to the consensus tree (Fig. 4f), such that Saurischia, consisting of only Sauropodomorpha and Herrerasauridae, diverged from Ornithoscelida, the clade uniting Theropoda and Ornithischia. *Eoraptor* was here noted as the earliest diverging taxon of Theropoda. Because the phylogenetic reconstruction as proposed by Baron et al., (2017) still

remains contested (Langer, et al., 2017), we reserve the use of the traditional reconstruction by Seeley (1887) as a basis for testing alternate placements of Silesauridae, Herrerasauridae, *Eoraptor*, and *Archaeopteryx*, until the phylogenetic reconstruction by Baron et al., (2017) has been discussed and tested further in the literature.

The six phylogenetic trees were exported as .phy files for subsequent analysis in R (V3.1.1). Since all theropods other than *Coelophysis* and *Herrerasaurus* were trimmed from the tree in sauropodomorph-specific analysis, alternative placement of *Archaeopteryx* (Fig. 4e) was only used in theropod-specific and pan-saurischian analyses.

Does body size predict osteological characters?

Phylogenetic logistic regression (PLR) was used to test the association between body size and discrete hip joint characters while accounting for phylogenetic relationships (Ives and Garland, 2010). Data were analyzed in R (Version 3.1.1) using the packages ape (Paradis et al., 2004) and phylolm (Ho et al., 2014), with femur length as the independent variable.

Each discrete character was tested for its association with log femur length using the Comparative Analysis with Generalized Estimating Equations function (compar.gee; Paradis and Claude, 2002). We tested the association between discrete characters and body size in the sauropod and theropod lineages. A number of osteological characters are acknowledged to be non-independent from each other. For example, a taxon with concentrated rugosities on the femoral head growth plate region needs to possess a rugose subchondral growth plate. A test of association between pairs of discrete characters is beyond the scope of the current study. Therefore, we analyzed the relationship between each discrete character and body size independently of other discrete characters.

Does body size predict hip joint dimensions?

Phylogenetic reduced major axis regression (PRMA) was used to test the relationship between body size and continuous hip joint characters while accounting for phylogenetic relationships (Butler and King, 2004; Revell, 2012). Data were analyzed in R (Version 3.1.1) the statistical packages *ape* (Paradis et al., 2004), *caper* (Orme, 2013), *pgls* (Mao and Ryan, 2012), and *phytools* (Revell, 2012), with femur length as the covariate. Pairs of characters were tested for association via *compar.gee* and for scaling relationship via *phyl.RMA*.

Allometric changes in femoral shape were assessed by the scaling relationships between the width and height of the femoral head, as well as *facies articularis antitrochanterica* (FAA) length. Allometric changes in acetabular shape were assessed by the scaling relationships between the depth, height, and length of the acetabulum. We identified allometric changes in the linear congruence of the bony hip joint by comparing each femoral linear metric with its corresponding acetabular metrics. Additionally, we assessed allometric changes in the composition of articular soft tissue using attachments' surface areas.

Allometric changes in hip joint bony congruence were assessed by scaling relationships between total femoral subchondral surface and the acetabular fossa. Allometric changes in femoral fibro- and hyaline cartilage attachments were calculated by scaling relationships between the metaphyseal collar and the growth plate. Allometric changes in acetabular tissue attachment surfaces were quantified by scaling relationships between the acetabular fossa, the bony acetabulum, and the supraacetabulum. Additionally, we measured the surface area of the ilial antitrochanter in order to incorporate taxa in which the ilium is the only preserved acetabular element. We identified allometric changes in surface area congruence of the bony hip joint by comparing each femoral surface area metric with its corresponding acetabular metric. For linear dimensions, we inferred isometric scaling if the regression slope did not differ significantly from 1. For surface area metrics, we inferred isometric scaling if the

regression slope did not differ significantly from 2. Positive and negative allometry was inferred respectively if the regression slopes was significantly greater or less than the isometric value.

Estimates of hip joint cartilage thickness in gigantic saurischians

We reconstructed the the proximal femoral cartilages thickness in two exemplary gigantic saurischians, *Tyrannosaurus rex* (FMNH PR 2081) and *Apatosaurus sp.* (= *Brontosaurus*, *sensu* Tschopp et al., 2015; FMNH P25115). We used cartilage correction factors (CCFs) described by Holliday et al. (2010) for *Alligator*, juvenile *Struthio*, and adult *Struthio* to estimate the thickness of femoral epiphyseal cartilage, and based the inference on similarity in growth plate morphology. Both taxa were given maximum and minimum estimates of cartilage thickness where applicable. The lack of quantitative data in extant archosaurs precludes thickness estimates for the acetabular labrum and antitrochanter cartilage. Instead, discrete osteological correlates were used to infer their acetabular soft tissue morphology (See Appendix S1).

RESULTS

Few osteological characters associate with body size

Results of the phylogenetic logistic regression are summarized in Tables 3 to 6 and Fig. 9. Among saurischians, only a few osteological correlates for hip joint articular soft tissues were predicted by body size. Within the sauropod lineage, rugosities on the proximal femoral growth plate (8) were positively associated with body size (Table 3). However, phylogenetic logistic regression was unable to determine the association of ilial ischial peduncular shape (5) and capitular concentration of irregular growth plate rugosities (9) with body size. These two characters underwent only one transition to the derived state within the

sauropod lineage, and the derived state was maintained throughout the Sauropodomorpha (Tsai et al., 2018). Moreover, the sauropodomorph taxa in the current study included only two evolutionary trends towards large body size within Plateosauridae and Anchisauridae. Therefore, the number of iterative transitions in the state of these characters was insufficient to determine their association with body size using phylogenetic logistic regression. In particular, the evolution of a cranially concave ischial peduncle of the ilium (5), concentrated irregular rugosities on the femoral head (9), transphyseal striations (10), and metaphyseal collar expansion (14) preceded evolutionary increase in body size, because these characters present the derived state in both small, early taxa and gigantic, later taxa. Overall, the hip joint morphology of sauropods was highly conserved throughout their evolutionary history. All alternative tree topologies returned statistically identical results as the consensus phylogenetic tree (Table 5).

Within the theropod lineage, no hip joint osteological characters showed significant associations with body size (Table 4). Phylogenetic logistic regression was unable to determine the association of proximal femoral growth plate rugosities (8) and ischiofemoral ligament sulcus depth (12) with body size. Rugosities are absent on the femoral growth plate of theropods along the stem lineage leading to birds but are present in both large-bodied theropods (e.g., *Tyrannosaurus*, *Allosaurus*, *Ceratosaurus*) as well as several smaller forms (e.g., *Ornithomimus*, *Anzu*, *Deinonychus*). Furthermore, Maniraptoriformes with rugose growth plates and shallow ischiofemoral ligament sulci are bracketed by those retaining smooth growth plates and deep sulci.

The sporadic occurrence of these derived character states within theropods indicates that multiple lineages independently evolved thick epiphyseal cartilages and fused pubofemoral and ischiofemoral ligaments (Tsai et al., 2018), regardless of body size

transitions. Overall, although sauropods and multiple lineages of gigantic theropods had thick layers of hyaline cartilage, evolutionary transitions in hip joint soft tissues were unassociated with body size transitions in either lineage. All alternative tree topologies returned statistically identical results as the consensus tree (Table 6).

Large saurischians possess absolutely greater hip joint soft tissues

Results of the phylogenetic reduced major axis regression using the “consensus” tree is summarized in Table 7 and 8 and illustrated in Fig. 5 to 8, whereas results from the five alternative tree topologies are summarized in Tables S3-11. Within the saurischian lineage, hip joint dimensions scaled with overall positive allometry relative to femur length, suggesting that large saurischians possess relatively larger bony hip joints than would be predicted by femur length. However, substantial overlap in confidence intervals between corresponding metrics indicated that the regression slopes did not differ significantly from each other (Tables S3-11). Since the relative dimensions of the subchondral (bony) femoral and acetabular surfaces remained consistent across the body size spectrum, large saurischians are inferred to have had proportionally similar, but absolutely greater, volumes of soft tissues in their hip joints.

Large saurischians possess greater amount of fibrocartilage on the femoral head

The largest sauropods and theropods used absolutely greater amounts of cartilage to construct their proximal femoral articular surfaces than their smaller relatives. With the exception of pennaraptorans (Oviraptorosauria + Paraves, Foth et al., 2014), all saurischians retained the ancestral dinosauriform morphology in possessing a distinct metaphyseal collar surrounding the subchondral growth plate surface on the proximal femur. The metaphyseal collar serves as the bony attachment surface for the fibrocartilage sleeve peripheral to the

hyaline cartilage core. The lack of a distinct metaphyseal collar necessitated the exclusion of pennaraptorans from the analyses of metaphyseal collar surface area. Nevertheless, in both sauropodomorphs and non-pennaraptoran theropods, the metaphyseal collar surface scaled to positive allometry relative to femur length. The scaling pattern of the metaphyseal collar surface area did not differ significantly from that of the subchondral growth plate, suggesting that gigantic saurischians used similar proportions but greater absolute amounts of fibro- and hyaline cartilage to build their hip joint as their smaller relatives. This morphology indicates that the entire ventral half of the femoral head's articular surface in gigantic theropods and sauropods consisted of a robust sleeve of fibrocartilage. Alternative tree topologies returned statistically identical results as the consensus phylogenetic tree.

Femoral and acetabular cartilages of gigantic sauropods

Sauropods possessed extremely thick layers of epiphyseal hyaline cartilage on the highly convoluted, irregularly rugose growth plates on their femoral heads. Using cartilage correction factors derived from extant archosaurs (Holliday et al., 2010), we reconstructed the proximal femoral epiphyseal cartilage in an *Apatosaurus* with an 1801 mm long femur, a 224 mm tall bony femoral head, and a 660 mm tall acetabulum. The minimal femoral cartilage thickness is inferred to have been 57.6 (± 20.2) mm based on the cartilage correction factor of the juvenile *Struthio*. Even with this minimal thickness reconstruction, the femoral head remained ellipsoid in medial view and must have articulated with a largely circular bony acetabulum. The acetabular “ceiling” of sauropods supported a fibrous acetabular labrum, as it lacks osteological correlates of thick hyaline cartilage. In order to maintain hip articulation under the minimal femoral cartilage thickness, the labrum would have been 378 mm thick. In contrast, the maximal thickness reconstruction assumed negligible thickness for the acetabular labrum (Fig. 9b), and estimated 436 mm of epiphyseal cartilage on the proximal

femur based on height congruence between the bony femoral head and the acetabulum, in order for the functional, cartilage-capped femoral head to fill the acetabulum.

Although the loading conditions of sauropod articular cartilage and acetabular labrum are unknown, we inferred the maximal femoral cartilage thickness estimate as the more mechanically plausible reconstruction. The minimal and maximal estimates of articular cartilage thickness suggested profound mechanical differences between the two reconstructions. Under the minimal estimate, the ellipsoid femoral head remained incongruent with the sub-circular bony acetabulum, such that the acetabular labrum must occupy the remainder of the joint space. During femoral protraction and retraction, the femoral head is inferred to have compressed against the labrum unequally, resulting in substantial deformation in the labrum. In contrast, the maximal estimate (the acetabulum-filling model) reconstructed the femoral head as a largely spherical articular surface, in which the dorsal hemisphere is formed by hyaline cartilage (Fig. 9b). Among non-mineralized skeletal tissues, hyaline cartilage is more resistant to compression compared to fibrous tissues (Freemont and Hoyland, 2006), thus would serve as a better load-bearing structure than the fibrous acetabular labrum. Moreover, the hyaline cartilage core of sauropods would have been surrounded on three sides by the fibrocartilage sleeve. The fibrocartilage sleeve has been hypothesized to provide additional mechanical support against avulsion and excessive deformation of the hyaline cartilage core (Tsai and Holliday, 2015). These lines of evidence indicate that the maximal cartilage thickness estimate provided a hip joint more suitable for compressive load bearing and was associated with the evolution of graviportal locomotor behavior. Therefore, the maximal cartilage thickness estimate is preferred over the minimal reconstruction scheme based on the cartilage correction factor of juvenile *Struthio*.

Gigantic sauropods used relatively small amounts of acetabular labrum and antitrochanter cartilages for maintaining hip joint articulation (Fig. 6d, e, h). Within the sauropod lineage, most hip joint metrics scaled with positive allometry relative to femur length. However, the regression slopes for labral attachment area, total bony antitrochanter surface area, and ilial bony antitrochanter surface area did not differ significantly from isometry. The attachment surface for the acetabular labrum and the antitrochanter cartilage increased at a lesser rate than other hip joint dimensions relative to femur length. Therefore, we inferred a trend of reducing supraacetabular soft tissue attachment during the evolution of sauropod gigantism (Table 8).

Femoral and acetabular cartilages of gigantic theropods

The most apparent anatomical transitions in the theropod hip joint were the reversion from a ventrolaterally oriented supraacetabular rim in early theropods to a laterally oriented supraacetabular rim in Avetheropoda (Britt, 1991; Zhao et al., 2009; Benson, 2010; Allain et al., 2012; Tsai et al., 2018), as well as the evolution of a more medially deflected femoral head within Avetheropoda (Allosauroidea + Coelurosauria), culminating in a fully medially deflected femoral head in Coelurosauria (Carrano, 2000; Hutchinson, 2001a). These morphologies have led to numerous skeletal reconstructions of coelurosaurs, and sometimes non-coelurosaurian avetheropods (e.g., *Allosaurus*, Bates et al., 2012) with a hinge-like hip joint articulation, in which the femoral head inserts into the acetabulum medially, perpendicular to the craniocaudal axis of sacrum (e.g., Hotton, 1980; Gatesy et al., 2009; Sellers, 2017). Under this orientation, the lack of dimensional congruence is apparent between the femoral head and the acetabular fossa. However, present inference of hip joint soft tissue anatomy questions the traditional reconstruction (Supplementary video 1) and argues that avetheropods retained a craniomedially oriented femoral head articulation

(Supplementary video 2). In other words, the avetheropodan femur may have typically been held rotated somewhat externally (laterally) about its long axis, as in extant birds (e.g. Kambic et al., 2014), to properly engage with the antitrochanter and acetabulum (see also figure 2 in Hutchinson and Allen, 2009; Bishop et al., 2018; and Tsai et al., 2019 for more discussion). This reconstruction reduces the craniocaudal incongruence between the femur and the acetabulum, and may have profound implications for the evolution of hip joint motion in theropods.

Although growth plate rugosities occur sporadically among nonavian theropods regardless of body size, gigantic theropods possessed absolutely thicker epiphyseal cartilage compared to their more basal relatives. When present, the level of growth plate rugosities of theropod femora never achieved the same level of convoluted texture as in the femoral heads of sauropods. Moreover, unlike in sauropods, the rugosities on theropod growth plates are more evenly distributed across the growth plate surface and largely take the form of transphyseal striations oriented perpendicular to the capitular-trochanteric axis. These observations suggest that theropod epiphyseal cartilages were thinner than the maximal estimate for sauropod femoral head cartilage (the acetabulum-filling model), and that theropods possessed a more evenly distributed cartilage thickness across the femoral head and trochanteric region.

Epiphyseal cartilage reconstructions for theropods were based on cartilage correction factors from *Struthio* and *Alligator* (Holliday, et al., 2010). For a 1280 mm *Tyrannosaurus* femur, the minimal estimate was 40.3 (± 10.6) mm of hyaline cartilage on the proximal femur; whereas the maximal estimate was 41.0 (± 14.4) mm. The cartilage thickness estimates here represent the most phylogenetically constrained attempt to date at non-avian theropod

epiphyseal anatomy. The overall similarities between *Struthio* and *Alligator*-based estimates suggest that both techniques are adequate for reconstructing cartilage thickness in theropods.

Gigantic theropods possessed absolutely and relatively greater amounts of acetabular labrum and antitrochanter fibrocartilage in the hip joint than their smaller relatives (Fig. 7, 8), as indicated by the positively allometric scaling trends in both labrum and antitrochanter attachment surface areas (Fig. 8d, h). These results indicate that the acetabular labrum and antitrochanter cartilage contributed significantly to hip joint articulation across the theropod body size spectrum and that both supraacetabular structures contributed appreciably to hip joint articulation during theropod evolution (Table 7).

DISCUSSION

Large theropods and sauropods independently evolved highly incongruent bony hip joints (Fig. 9a), in which articulation was maintained by thick layers of soft tissues (Fig. 9b, c). However, differences in the patterns of character state transitions between the two lineages indicate that large sauropod and theropod hip joints had fundamentally different morphologies. This study used phylogenetic comparative methods to test the relationship between body size, articular soft tissue composition, and hip joint dimensions of saurischians. Only a few hip joint characters in the analysis showed correlated evolution with body size transitions in saurischians. Moreover, most bony hip joint metrics of saurischians scaled with positive allometry, but the allometric relationships scaled similarly to each other. This indicates that the proportional contribution of hip joint soft tissue remained consistent while the overall amount of soft tissue increased with positive allometry across the body size spectrum in Saurischia. As neither bony nor soft tissues of the hip joint scaled with sufficient allometry to maintain constant area vs. body size (e.g., mass) ratios, larger saurischians would have had to alter their limb mechanics to avoid increasing peak tissue stresses. Potential

alterations would include slower maximal speeds, more vertically oriented limbs and loss of running gaits; all of these most likely to be prevalent in giant sauropods (and to a degree, theropods), and paralleling patterns in other large tetrapods (e.g., Alexander, 1985; Biewener, 1990; Sanders et al., 2011; Sellers et al., 2013).

The highly cartilaginous sauropod femoral head in the evolution towards graviportality

Sauropodomorphs evolved medially deflected, highly cartilaginous femoral head regions during the late Triassic, prior to their massive evolutionary increase in body size (Sereno, 1997; Sander et al., 2004; Rauhut et al., 2011; Otero and Pol, 2013; Tsai et al., 2018). In particular, sauropods possessed enormous amounts of hyaline cartilage on the femoral head (capitular region), up to 436mm in *Apatosaurus*, to maintain articulation with a highly reduced acetabular labrum (Fig. 9b). In contrast, isometric scaling patterns of the attachment surfaces of the labrum and the antitrochanter indicate that sauropodomorphs reduced these soft tissues relative to other articular soft tissues, as well as overall hip joint dimensions, during evolutionary increases of body size. Reduction of the antitrochanter resulted in a largely circular outline for the acetabulum, which articulated with the spherical outline of the cartilaginous femoral head (Fig. 9b). Sauropodomorphs reduced the ancestral femoral neck-antitrochanter articulation during their evolutionary increase in body size. Instead, the cranially oriented antitrochanter formed the caudal limit of the hip joint capsule, and constrained the femoral head inside the acetabulum.

Femur length was a significant predictor for the presence of thick hyaline cartilage on the femoral head of the dinosauromorph lineage leading to sauropods. Evolutionary increase in body size occurred multiple times in the sauropod lineage: once within early dinosauromorphs and twice among sauropodomorphs. Among early dinosauromorphs, silesaurids evolved larger body size compared to lagerpetids and *Marasuchus* (Turner and

Nesbitt, 2013), whereas sauropodomorphs underwent multiple increases in body size along the lineage leading to sauropods (Yates, 2004; Sander et al., 2011). Small-bodied sauropodomorphs had markedly different growth plate morphology compared to their larger relatives. The small-bodied *Adeopapposaurus* possessed smooth subchondral growth plates, and smooth subchondral growth plates have also been reported for the small-bodied *Pampadromaeus* (Müller et al., 2015) and *Saturnalia* (Langer, 2003). In contrast, thick hyaline cartilage was present in plateosaurids and the common ancestor of *Mussaurus* and sauropods. Thick hyaline cartilage has been hypothesized by Holliday et al (2010) to function as a reservoir for growth plate cartilage in dinosaurs. Thickness of the hyaline and calcified cartilage layer at the terminal ends of avian femora is positively associated with the rate of longitudinal growth (Thorp, 1988; Montes et al., 2005). Thus the independent gains of thick cartilage in silesaurids and sauropodomorphs may indicate faster longitudinal limb growth rates or longer growth periods.

Sauropodomorphs retained the basal dinosauriform morphology of an expanded metaphyseal collar, indicative of a well-developed bony attachment for the fibrocartilage sleeve. Fibrocartilage is more resistant to tensile and translational shear loads than hyaline cartilage (Schinagl et al., 1997; Freemont and Hoyland, 2006); thus the presence of fibrocartilage on the periphery of the femoral head provided additional mechanical support against avulsion of the thick epiphyseal hyaline cartilage layer during femoral excursion. Additionally, the fibrocartilage may also increase the axial compressive resistance of the femoral head hyaline cartilage. Since hyaline cartilage is weaker in its compressive resistance compared to bone, a purely hyaline epiphyseal cartilage would undergo axial deformation under compressive loads, decreasing in dorsoventral height and overfilling the periphery of the subchondral growth plate. The fibrocartilage sleeve may serve to limit the extent of such

deformation by acting as an inextensible sleeve around the hyaline cartilage core, analogous to the function of the annulus fibrosus in the intervertebral discs in mammals (Markolf and Morris, 1974). Therefore, although the evolutionary gain of an extensive fibrocartilage sleeve preceded gigantism in sauropodomorphs, retention of this ancestral Dinosauriformes character state may have facilitated the increase in hyaline cartilage thickness. Therefore, the fibrocartilage sleeve was an important trait which facilitated the evolution of sauropod gigantism.

The epiphyseal hyaline cartilage layer of silesaurids and sauropodomorphs differed in absolute thickness and attachment morphology on the subchondral growth plate, likely associated with the absolute magnitude of body size. The largest silesaurids reached up 345 mm (NHMUK R16303, Barrett et al., 2014) in femur length and are estimated to possess up to 28.5 mm of epiphyseal hyaline cartilage at the proximal femur (Tsai, 2015). Among silesaurids, the epiphyseal hyaline cartilage attached to the subchondral growth plate via a cartilage cone surrounded by shallow (<1 mm), irregular rugosities. Although the cartilage cone was variably present in early sauropodomorphs, it was absent in sauropods. Instead, the sauropod hyaline cartilage core attached to the subchondral growth plate via highly convoluted rugosities up to 20 mm in amplitude. The evolutionary transition of the metaphyseal growth plate from a cartilage cone-dominated articulation to a rugosities-dominated articulation may have been associated with need for the extremely thick layer of hyaline cartilage to resist shear forces during femoral protraction and retraction. Compared to the cartilage cone-trough articulation, the highly convoluted rugosities on the growth plate provided a highly interdigitated junction between the hyaline and calcified cartilage layers at the growth plate. Therefore, the highly rugose growth plate on the sauropod femoral head may have functioned to increase the amount of frictional grip between the two tissues under

locomotion-induced translational and rotational shear loads, and to prevent slippage and avulsion of the thick cartilage cap. Overall, our results indicate that sauropodomorphs evolved highly divergent hip joint morphology among dinosaurs during the Triassic-Jurassic transition. This study is not dependent on the novel reconstruction of dinosaur phylogeny by Baron et al. (2017) because we have focused on hip-specific anatomical characters, included only a small number of ornithischians as outgroup taxa, and our results were relatively insensitive to the phylogeny used. Nevertheless, it is evident that in contrast to the more anatomically conservative hip joints of theropods and ornithischians, the sauropod hip joint underwent numerous novel changes that predated their evolution of gigantism.

Theropod hip joints underwent clade-specific transitions during body size evolution

Gigantic theropods possessed hip joints with extensive amounts of supraacetabular articular pads, as well as contact between the femoral neck and the antitrochanter (Fig. 9c). Evolution of the theropod hip joint was characterized by a high level of phylogenetic signal, which complicates inferences of character transitions associated with gigantism. Among theropods, the osteological correlates of articular soft tissues cannot be reliably predicted by femur length; whereas all hip joint dimensions scaled to overall positive allometry relative to femur length. These results indicate gigantic theropods had overall similar types, distribution, and proportions of hip joint soft tissues as their smaller relatives. However, as in the sauropod lineage, dimensional similarity in the bony hip joint across the theropod body size spectrum indicated absolutely thicker layers of articular soft tissue in gigantic taxa. This inference is consistent with the presence of rugose subchondral growth plates on the proximal femur of the largest theropods. Although the rugosities on the theropod proximal femur never approached the same level of convoluted texture as in sauropods, reconstructed cartilage thickness using cartilage correction factors (Holliday et al., 2010) nevertheless indicate that

large theropods possessed epiphyseal cartilage layers both relatively and absolutely thicker than those of mammals and most extant birds.

In theropods, the surface areas of the acetabular labrum and antitrochanter scaled to positive allometry relative to body size, contributing to the overall bony overlap between the femur and the acetabulum. Since these two surface areas provided attachment for the acetabular labrum and antitrochanter cartilage, respectively, large theropods are inferred to have used large amounts of supraacetabular soft tissues in addition to thick layers of femoral epiphyseal cartilage in maintaining hip joint congruence. Unlike sauropods, theropods maintained the ancestral diapsid hip joint articulation (Tsai and Holliday, 2015), in which the femoral head (capitular region) articulates with the acetabular labrum and the fibrocartilaginous surface femoral neck (trochanteric region) articulated with the antitrochanter at the caudal acetabulum (see also Hutchinson and Allen, 2009). Moreover, theropods show distinct osteological correlates for intracapsular ligaments at the femoral head region. However, the current analysis of this ligament osteological correlates was limited by coding them as binary characters-- the depth, width, and angle of the sulcus likely varied along a continuous spectrum among different clades. Nevertheless, our results suggest that the femoral head was constrained within the cranial acetabular fossa and acted as a fulcrum during femoral motion. In contrast, the fibrocartilaginous surfaces of the femoral neck and antitrochanter likely resisted translational shear loading during femoral axial rotation, as in extant birds (Kambic et al., 2014). The antitrochanters of non-avian theropods tended to maintain an open synchondrosis, rather than being ossified as in extant birds. The open synchondrosis morphology allows a substantial volume of hyaline cartilage core, deep to the superficial layer of fibrocartilage spanning the ilial and ischial peduncles. Although this morphology is present in non-avian theropods across the body size spectrum, the presence of

an extensive hyaline cartilage core in the antitrochanter may have provided additional load-bearing abilities in large theropods, serving as a pliant articular pad of constant volume against the femoral neck.

The theropod hip joint underwent transitions in the orientation of the supraacetabular rim and the femoral head, but neither of these characters varies predictably with body size. Early theropods possessed a ventrolaterally oriented supraacetabular rim, but the rim shifted to a fully lateral orientation in Avetheropoda and maintained this position throughout the avian stem lineage (Tsai et al., 2018). Similarly, theropods ancestrally had a craniomedially oriented femoral head, whereas avetheropods shifted to a more medially deflected femoral head. Medial deflection of the femoral head is here analyzed as a binary character, but the actual transition likely occurred along a continuum within the theropod lineage. Moreover, the presence of megalosaurids with more medially deflected femoral heads (e.g., *Megalosaurus* with 20° deflection; Benson, 2010), as well as coelurosaurians (e.g., *Zuolong*, Choiniere et al., 2010) and allosauroids with craniomedially oriented femoral heads (e.g., *Neovenator*, Brusatte et al. 2008) suggest that the evolution of a fully medially deflected femoral head in theropods was not a straightforward process, but likely resulted from multiple, independent acquisitions within different lineages. Nevertheless, morphology of the supraacetabular rim and femoral head orientation tend not to differ between gigantic theropods and their small relatives. For example, the large Jurassic megalosauroid *Torvosaurus* retains a ventrolaterally oriented supraacetabular rim, similar to smaller Triassic-Jurassic theropods such as *Coelophysis* and *Dilophosaurus*. In contrast, the supraacetabular rim and femoral head orientation of *Tyrannosaurus* did not differ from the compsognathids (e.g., *Compsognathus*, Ostrom, 1978; *Sinosauropteryx*, Currie and Chen, 2001; *Sinocalliopteryx*, Ji et al., 2007), suggesting similar hip joint articulation among these

closely related coelurosaurian taxa. Overall, the thickness of theropod hip joint articular soft tissue thickness was heavily influenced by body size. In contrast, the lack of association between body size and other hip joint characters indicates that the theropod hip joint underwent clade-specific transitions, and was more influenced by factors such as the step-wise acquisition of avian-like body shape (Hutchinson 2001a; Allen et al., 2013) and locomotor posture (Hutchinson and Allen, 2009) at each node along the stem lineage.

Dorsally inclined proximal femora and their implications for epiphyseal morphology

In many saurischians, the proximal femur is dorsally inclined, such that the femoral head is elevated relative to the femoral midshaft. This morphology is by far most prevalent in large bodied sauropods (Bonnar 2010, 2013; Carrano, 2005) and some large-bodied theropods (tyrannosauroids, Hutchinson, 2001a, Bishop et al., 2018; carcharodontosaurians, Canale et al., 2015). Femoral head inclination has also been hypothesized to be an adaptation for gigantism in sauropods (Wilson and Carrano, 1999) and theropods (Bates, 2012a). However, dorsally inclined proximal femora are also present in smaller saurischians, such as oviraptorosaurs (*Khaan*, Balanoff and Norell, 2014; *Anzu*, Lamanna et al., 2014), small-bodied sauropods (*Magyarosaurus*, Stein et al., 2010), and some extant birds (e.g., *Struthio* and *Rhea*, Tsai and Holliday, 2015). Whereas previous work tends to address this morphology as a bivariate character (Stovall and Langston, 1950; Wilson and Sereno, 1995), this study found that proximal femoral elevation can be achieved in multiple ways among saurischians. Among large theropods, oviraptorosaurs and extant birds, the femoral head is markedly convex relative to the metaphyseal line, such that the dorsal inclination of the proximal femur is largely attributed to the sub-spherical growth plate surface on the femoral head. In contrast, the proximal femur of *Nothronychus* (UMNH VP 16420) is inclined dorsally by both femoral head convexity as well as the dorsal tilting of the femoral neck.

Moreover, the growth plate surfaces of *Allosaurus* (UMNH VP 2560; DMNH 44397; FMNH P 25114), some tyrannosaurids (IGM 100-1844; RAM 9132; UMNH VP 16690), and *Ornithomimus* (RAM 6794) are only slightly convex relative to the metaphyseal line, instead achieving dorsal inclination via dorsal tilting of the femoral neck and the expanded metaphyseal collar. Thus the dorsal inclination of the theropod femoral head may have been associated with differences in the distribution of fibro- and hyaline cartilage attachments on the femoral head, as well as extent of ossification of the subchondral surface.

Sauropods evolved dorsally inclined proximal femoral heads in several ways. Among sauropods, macronarians possessed a wide range of femoral head morphologies.

Camarasaurus (DNM 4514), *Sauroposeidon* (YPM 5449), and *Cedarosaurus* (DMNH 37045) achieved dorsal inclinations of the proximal femur via highly convex subchondral surfaces on the femoral head. The convex femoral heads of *Camarasaurus* and most other macronarians likely supported thinner layers of epiphyseal hyaline cartilage compared to those of diplodocoids and titanosaurs. In contrast, *Brachiosaurus* (FMNH P25107), *Giraffatitan* (MB.R. 2694, 2181.83, 5016), and *Argyrosaurus* (FMNH P13019) possessed less convex growth plates on the femoral head, similar to the early sauropod *Patagosaurus* (MACN 1986) and the sauropodomorph *Mussaurus* (MLP MLP 60-III-20-22). Dorsal inclinations of the femoral head in these taxa were achieved by increased femoral neck angle relative to the midshaft long axis. Moreover, *Alamosaurus* (TMM 41541) and *Rapetosaurus* (FMNH PR 2209) possessed similar femoral head morphology as *Argyrosaurus* but had laterally deflected femoral midshaft and beveled distal condyles (Wilson and Carrano, 1999). Finally, diplodocoids such as *Barosaurus* (NAMAL 106), *Diplodocus* (CM 84; DMNH 462), and *Apatosaurus* (CM 85, 3018; FMNH 25112) possess largely planar subchondral growth plates on the femoral head, but the rugosities in this region appear to be greater than those of

macronarians in amplitude and surface area. *Dicraeosaurus* (MB.R. 2692, 2695), *Barosaurus* (NAMAL 106) and *Tornieria* (MB.R. 2671) exhibit dorsally elevated, but not inclined, femoral heads compared to the trochanteric region, similar to *Brachiosaurus*, *Giraffatitan*, and *Argyrosaurus*. However, unlike macronarians, the subchondral surfaces of these diplodocoids remain largely planar and replete with highly convoluted rugosities, even among sauropods. The combination of these osteological correlates indicates that diplodocoids also evolved a dorsally inclined femoral head, albeit one comprised largely of hyaline cartilage. Results of this study show that the dorsal inclination of the bony femoral head in sauropods was attained by multiple morphologies, including differential level of cartilage thickness, growth plate ossification, and femoral neck-to-midshaft angles. The dorsally inclined proximal femur of titanosaurs has been associated with wide-gauge sauropod trackways, and is inferred to be an adaptation for increased graviportal locomotor behaviors (Wilson and Carrano, 1999). Nevertheless, interaction between femoral neck-to-midshaft angles, articular cartilage thickness, and ligamentous constraints remain unknown in sauropods. Overall, the variation in femoral head dorsal inclination suggests a wide range of femoral articular morphology among sauropods. Despite the early, concerted evolutionary transition into graviportal locomotion, the morphological diversity of sauropod hip joints potentially indicates a spectrum of epiphyseal cartilage thickness, load bearing mechanics, joint dynamics, and growth strategies within this clade of gigantic archosaurs.

Evolution of epiphyseal cartilage in bird-like theropods

The evolution of cartilage thickness, type, and distribution in Maniraptoriformes is of interest due to the wide spectrum of body size in this clade. Gigantic body size (>2 tons) independently evolved in ornithomimosaurs (*Deinocheirus*, Lee et al., 2014a), therizinosaurus (*Therizinosaurus*, Barsbold, 1976), and oviraptorosaurs (*Gigantoraptor*, Xu et al., 2007).

Although paravians never evolved similar magnitudes of gigantic body size, deinonychosaurs (*Utahraptor*, Kirkland et al., 1993; *Achillobator*, Perle et al., 1999), and Neornithes/Aves (*Aepyornis*, Anderson et al., 1979; Dinornithidae, Bunce et al., 2003) nevertheless produced moderately large taxa (~500 kg for *Aepyornis*, Amadon, 1947; up to 700-1000 kg for *Utahraptor*, Peczki, 1994). The relationship between hip joint morphology and body size within Maniraptoriformes, in particular pennaraptorans, is difficult to interpret due to the lack of well-preserved hip joints of gigantic taxa in this study. Among well-preserved Maniraptoriformes included in this analysis, *Ornithomimus* (RAM 14182), *Anzu* (CM 78000) and *Deinonychus* (MCZ 4371) possess rugose femoral growth plates indicative of thick hyaline cartilage but are bracketed by taxa possessing smooth femoral growth plates (Tsai et al., 2018). Although these three taxa are moderately large for their respective clades, they are within the lower end of the body size spectrum among non-avian theropods (Turner et al., 2007). Therefore, the association between hyaline cartilage thickness and body size remains difficult to infer without additional samples of large-bodied Maniraptoriformes.

Moreover, pennaraptorans exhibit a continuous subchondral growth plate surface without a distinct metaphyseal collar. This morphology is the osteological correlate for a bird-like distribution of femoral epiphyseal cartilages, in which the fibrocartilage sleeve possesses little bony attachment on the metaphysis, and forms the articular surface of the proximal femur by completely encapsulating the hyaline cartilage core (Tsai, 2015). The evolution of the composite fibro-hyaline cartilage core within Pennaraptora, its mechanical and ontogenetic role during the evolution of the stem avian lineage (Turner et al., 2007), as well as the evolution of determinate growth among extant birds (Erickson, 2005), remain poorly understood. The evolution of maniraptoriform hip joint anatomy thus remains an open avenue for future studies in locomotor and growth adaptations associated with independent

gain of gigantism and sustained miniaturization along the avian stem lineage (Turner et al., 2007).

Ontogenetic significance of hip joint cartilages thickness in saurischians

Most saurischians retained significant proportions of femoral epiphyseal cartilage and incompletely fused acetabulae. In extant birds, mammals, and lepidosaurs, thick epiphyseal cartilages (Haines, 1938), and unfused acetabulae (Cracraft 1986; Bolter and Zihlman, 2003; Conrad, 2006) occur in skeletally immature individuals. However, these characters were not used as ontogenetic indicators in the present study because most extinct saurischians retain these “unfinished” morphologies throughout ontogeny, even as reproductively mature, large-bodied adults (Brochu, 2003; Tidwell et al., 2005). Moreover, some extant sauropsids do retain thick hyaline cartilage layers and unfused girdle elements at adulthood (e.g., the proximal humerus of *Dermochelys*, Gervais, 1872; the anterior acetabular cartilage in crocodylians, Tsai and Holliday, 2015).

We hypothesize that saurischians underwent ontogenetic heterochrony during the evolution of its two major clades. Early dinosauromorphs had smooth subchondral growth plate surfaces and unfused antitrochanters, with independent transitions to the derived state in multiple saurischian lineages. The transitions from smooth to rugose femoral growth plates are indicative of paedomorphosis (retention of juvenile ancestral traits in descendant adults). Studies in dinosaur growth dynamics have shown that non-avian dinosaurs maintained active skeletal growth after achieving sexual maturity (Padian et al., 2001; Erickson et al., 2007; Lee and Werning, 2008). Therefore, retention of the juvenile characteristics, such as a thick femoral epiphyseal cartilage and an unfused antitrochanter, likely facilitated the evolution of gigantism in sauropods and multiple lineages of theropods. In contrast, the independent evolution of antitrochanter ossification in theropods indicates peramorphosis (earlier

attainment, and thus enhancement, of adult traits), in which a co-ossified antitrochanter indicates cessation of acetabular growth. Although the antitrochanter remained an open synchondrosis in the sauropod and theropod stem lineage, it underwent transitions to the co-ossified state in *Herrerasaurus*, *Coelophysus*, Ceratosauria (except *Ceratosaurus*), and Avialae. Antitrochanter co-ossification shows no significant relationship with body size but appears to have co-occurred with smooth subchondral growth plates on the proximal femur, suggesting a possible relationship of overall cartilage thinning in these taxa. The independent evolution of acetabular co-ossification in theropods may have been influenced by specific transitions in growth dynamics, as well as load-bearing modalities at the caudal acetabulum.

CONCLUSION

The evolutionary history of saurischian dinosaurs was characterized by multiple, independent evolutionary transitions in body size, as well as a wide diversity of hip joint morphology and locomotor postures. In both sauropods and theropods, the largest taxa maintained hip joint congruence using articular soft tissues orders of magnitude thicker than those of mammals. In particular, gigantic sauropods possessed thicker layers of epiphyseal hyaline cartilage on the femoral head region than gigantic theropods, and maintained hip joint congruence primarily with the largely cartilaginous femoral head. In contrast, gigantic theropods maintained hip joint articulation using substantial contributions from the acetabular labrum and the antitrochanter cartilage. Nevertheless, the size of the hyaline cartilage core of gigantic theropod hips exceeded those of most extant vertebrates. Both theropods and sauropodomorphs used an extensive fibrocartilage collar as mechanical support for thick layers of hyaline cartilage core. These findings indicate that the femoral articular cartilages of giant sauropods were built to sustain heavy compressive loads whereas those of giant theropods experienced compression and translational shear forces. These data indicate that

saurischian hips underwent divergent transformations in soft tissue morphology reflective of body size, locomotor posture, and joint loading.

LITERATURES CITED

Alexander, R. M. 1985. Mechanics of posture and gait of some large dinosaurs. *Zoological Journal of the Linnean Society* 83(1), 1-25.

Allain, R., T. Xaisanavong, P. Richir, and B. Khentavong. 2012. The first definitive Asian spinosaurid (Dinosauria: Theropoda) from the Early Cretaceous of Laos. *Naturwissenschaften* 99, 369–377.

Allen, V., K. T. Bates, Z. Li, and J. R. Hutchinson. 2013. Linking the evolution of body shape and locomotor biomechanics in bird-line archosaurs. *Nature* 497:104–107.

Allen, V., H. Paxton, and J. R. Hutchinson. 2009. Variation in center of mass estimates for extant sauropsids and its importance for reconstructing inertial properties of extinct archosaurs. *Anatomical Record* 292:1442–1461.

Amadon, D. 1947. An Estimated Weight of the Largest Known Bird. *Condor* 49, 159–164.

Anderson, J. F., H. Rahn, and H. D. Prange. 1979. Scaling of Supportive Tissue Mass. *Q Rev Biol* 54, 139–148.

Anderson, J. F., A. Hall-Martin, and D. A. Russell. 1985. Long-bone circumference and weight in mammals, birds and dinosaurs. *Journal of Zoology* 207:53–61.

Balanoff, A. M., and M. A. Norell. 2012. Osteology of *Khaan mckennai* (Oviraptorosauria: Theropoda). *Bulletin of the American Museum of Natural History* 372:1–77.

Baron, M. G., D. B. Norman, and P. M. Barrett. 2017. A new hypothesis of dinosaur relationships and early dinosaur evolution. *Nature* 543:501–506.

Barnett, C. H. 1954. The structure and functions of fibrocartilages within vertebrate joints. *Journal of Anatomy* 88:363–368.

Barrett, P. M., S. J. Nesbitt, and B. R. Peacock. 2015. A large-bodied silesaurid from the Lifua Member of the Manda beds (Middle Triassic) of Tanzania and its implications for body-size evolution in Dinosauromorpha. *Gondwana Research* 27:925–931..

Barsbold, R. 1976. New data on *Therizinosaurus* (Therizinosauridae, Theropoda) [in Russian]. Pp. 212–232 in E. V. Devâtkin and N. M. Ânovskaâ, eds. *Paleontologiâ i biostratigrafiâ Mongolii*. Trudy, Sovmestnaâ Sovetsko–Mongol’skaâ paleontologiçeskaâ kspediciâ.

Bates, K. T., R. B. J. Benson, and P. L. Falkingham. 2012. A computational analysis of locomotor anatomy and body mass evolution in Allosauroidea (Dinosauria: Theropoda). *Paleobiology* 38:486–507.

Bates, K. T., S. C. R. Maidment, V. Allen, and P. M. Barrett. 2012. Computational modelling of locomotor muscle moment arms in the basal dinosaur *Lesothosaurus diagnosticus*: assessing convergence between birds and basal ornithischians. *Journal of Anatomy* 220:212–232.

Benson, R. B. J. 2010. A description of *Megalosaurus bucklandii* (Dinosauria: Theropoda) from the Bathonian of the UK and the relationships of Middle Jurassic theropods. *Zool J Linn Soc* 158, 882–935.

Benson, R. B. J., N. E. Campione, M. T. Carrano, P. D. Mannion, C. Sullivan, P. Upchurch, and D. C. Evans. 2014. Rates of dinosaur body mass evolution indicate 170 million years of sustained ecological innovation on the avian stem lineage. *PLoS Biol.* 12:e1001853.

Biewener, A. A. 1990. Biomechanics of mammalian terrestrial locomotion. *Science* 250(4984): 1097–1103.

Biewener, A. A. 1991. Musculoskeletal design in relation to body size. *Journal of Biomechanics* 24 Suppl 1:19–29.

Bishop, P. J., S. A. Hocknull, C. J. Clemente, J. R. Hutchinson, A. A. Farke, R. S. Barrett, and D. G. Lloyd. 2018. Cancellous bone and theropod dinosaur locomotion. Part III—Inferring posture and locomotor biomechanics in extinct theropods, and its evolution on the line to birds. *PeerJ* 6:e5777.

Bonnan, M. F., J. L. Sandrik, T. Nishiwaki, D. R. Wilhite, R. M. Elsey, and C. Vittore. 2010. Calcified cartilage shape in archosaur long bones reflects overlying joint shape in stress-bearing elements: Implications for nonavian dinosaur locomotion. *Anatomical Record* 293:2044–2055.

Bonnan, M. F., D. R. Wilhite, S. L. Masters, A. M. Yates, C. K. Gardner, and A. Aguiar. 2013. What lies beneath: sub-articular long bone shape scaling in eutherian mammals and saurischian dinosaurs suggests different locomotor adaptations for gigantism. *PLoS One* 8:e75216.

Bonnan, M. F. 2007. Linear and geometric morphometric analysis of long bone scaling patterns in Jurassic neosauropod dinosaurs: their functional and paleobiological implications. *Anatomical Record* 290:1089–1111.

Britt, B. 1991. Theropods of Dry Mesa Quarry (Morrison Formation, late Jurassic), Colorado, with emphasis on the osteology of *Torvosaurus tanneri*. *BYU Geology Studies* 37, 1–72.

Brown, J. W., J. S. Rest, J. García-Moreno, M. D. Sorenson, and D. P. Mindell. 2008. Strong mitochondrial DNA support for a Cretaceous origin of modern avian lineages. *BMC Biology* 6:6.

Brusatte, S. L., R. B. J. Benson, and S. Hutt. 2008. The osteology of *Neovenator salerii* (Dinosauria: Theropoda) from the Wealden Group (Barremian) of the Isle of Wight. *Monograph of the Palaeontographical Society* 162, 1–75.

Brusatte, S. L., M. J. Benton, J. B. Desojo, and M. C. Langer. 2010. The higher-level phylogeny of Archosauria (Tetrapoda: Diapsida). *Journal of Systematic Palaeontology* 8:3–47.

Brusatte, S. L., S. J. Nesbitt, R. B. Irmis, R. J. Butler, M. J. Benton, and M. A. Norell. 2010. The origin and early radiation of dinosaurs. *Earth Science Reviews* 101:68–100.

- Bunce, M., T. H. Worthy, T. Ford, W. Hoppitt, E. Willerslev, A. Drummond, and A. Cooper. 2003. Extreme reversed sexual size dimorphism in the extinct New Zealand moa *Dinornis*. *Nature* 425:172–175.
- Butler, M. A., and A. A. King. 2004. Phylogenetic Comparative Analysis: A Modeling Approach for Adaptive Evolution. *The American Naturalist* 164:683–695.
- Campione, N. E., and D. C. Evans. 2012. A universal scaling relationship between body mass and proximal limb bone dimensions in quadrupedal terrestrial tetrapods. *BMC Biology*, 10(1): 60.
- Carrano, M. T. 1999. What, if anything, is a cursor? Categories versus continua for determining locomotor habit in mammals and dinosaurs. *Journal of Zoology* 247:29–42.
- Carrano, M. T. 2000. Homoplasy and the evolution of dinosaur locomotion. *Paleobiology* 26:489–512.
- Carrano, M. T. 2001. Implications of limb bone scaling, curvature and eccentricity in mammals and non-avian dinosaurs. *Journal of Zoology* 254:41–55.
- Canale, J. I., F. E. Novas, D. Pol. 2015. Osteology and phylogenetic relationships of *Tyrannotitan chubutensis* Novas, de Valais, Vickers-Rich and Rich, 2005 (Theropoda: Carcharodontosauridae) from the Lower Cretaceous of Patagonia, Argentina. *Hist Biol* 27, 1–32.
- Carrano, M. T., R. B. J. Benson, and S. D. Sampson. 2012. The phylogeny of Tetanurae (Dinosauria: Theropoda). *Journal of Systematic Palaeontology* 10:211–300.
- Carter, D. R., and G. S. Beaupré. 2007. *Skeletal Function and Form: Mechanobiology of Skeletal Development, Aging, and Regeneration*. Cambridge University Press.
- Carter, D. 1998. Epigenetic mechanical factors in the evolution of long bone epiphyses. *Zoological journal of the Linnean Society* 123:163–178.
- Carter, D. R., and M. Wong. 2003. Modelling cartilage mechanobiology. *Philosophical transactions of the Royal Society B: Biological Sciences* 358:1461–1471.
- Christiansen, P. E. and R. A. Fariña. 2004. Mass Prediction in Theropod Dinosaurs. *Historical Biology* 16: 85–92.
- Choiniere, J. H., J. M. Clark, C. A. Forster, and X. Xu. 2010. A basal coelurosaur (Dinosauria: Theropoda) of the Shishugou Formation in Wucuiwan, People’s Republic of China. *Journal of Vertebrate Paleontology* 30: 1779-1796.
- Clarke, J. A., C. P. Tambussi, J. I. Noriega, G. M. Erickson, and R. A. Ketcham. 1997. Definitive fossil evidence for the extant avian radiation in the Cretaceous. *Nature* 385:333–338.
- Cope, E. D. 1878. On the Saurians Recently Discovered in the Dakota Beds of Colorado. *The American naturalist* 12:71–85.
- Cracraft, J. 1971. The functional morphology of the hind limb of the domestic pigeon, *Columba livia*. *Bulletin of the American Museum of Natural History* 144:175–268.

- Currie, P. J. and P. J. Chen. 2001. Anatomy of *Sinosauropteryx prima* from Liaoning, northeastern China. *Can J Earth Sci* 38, 1705–1727.
- de Buffrénil, V., I. Ineich, and W. Böhme. 2005. Comparative Data on Epiphyseal Development in the Family Varanidae. *Journal of Herpetology* 39:328–335. The Society for the Study of Amphibians and Reptiles.
- Enlow, D. H. 1969. The Bone of Reptiles. Pp. 45–80 in C. Gans, ed. *Biology of the Reptilia*. Academic Press, New York.
- Erickson, G. M., P. J. Makovicky, P. J. Currie, M. A. Norell, S. A. Yerby, and C. A. Brochu. 2004. Gigantism and comparative life-history parameters of tyrannosaurid dinosaurs. *Nature* 430:772–775.
- Erickson, G. M. 2005. Assessing dinosaur growth patterns: a microscopic revolution. *Trends in Ecology and Evolution* 20:677–684.
- Erickson, G. M., K. Curry Rogers, D. J. Varricchio, M. A. Norell, and X. Xu. 2007. Growth patterns in brooding dinosaurs reveals the timing of sexual maturity in non-avian dinosaurs and genesis of the avian condition. *Biology Letters*. 3:558–561.
- Ericson, P. G. P., C. L. Anderson, T. Britton, A. Elzanowski, U. S. Johansson, M. Källersjö, J. I. Ohlson, T. J. Parsons, D. Zuccon, and G. Mayr. 2006. Diversification of Neoaves: integration of molecular sequence data and fossils. *Biology Letters* 2:543–547.
- Ezcurra, M. D., T. M. Scheyer, and R. J. Butler. 2014. The origin and early evolution of Sauria: reassessing the Permian Saurian fossil record and the timing of the crocodile-lizard divergence. *PLoS One* 9:e89165.
- Falkingham, P. L. 2012. Acquisition of high resolution three-dimensional models using free, open-source, photogrammetric software. *Palaeontologia electronica* 15:15.
- Farlow, J. O., G. R. Hurlburt, R. M. Elsey, A. R. C. Britton, W. Langston. 2005. Femoral Dimensions and Body Size of *Alligator mississippiensis*: Estimating the Size of Extinct Mesoeucrocodylians. *Journal of Vertebrate Paleontology* 25, 354–369.
- Firbas, W., and K. Zweymüller. 1971. Über das Hüftgelenk der Ratiten. *Gegenbaurs Morphol. Jahrb.* 116:91–103.
- Foth, C., H. Tischlinger, and O. W. M. Rauhut. 2014. New specimen of Archaeopteryx provides insights into the evolution of pennaceous feathers. *Nature* 511:79–82.
- Freemont, A. J., and J. Hoyland. 2006. Lineage plasticity and cell biology of fibrocartilage and hyaline cartilage: its significance in cartilage repair and replacement. *European Journal of Radiology* 57:32–36.
- Gatesy, S. M., M. Bäker, and J. R. Hutchinson. 2009. Constraint-based exclusion of limb poses for reconstructing theropod dinosaur locomotion. *Journal of Vertebrate Paleontology* 29:535–544.
- Graf, J., Stofft, E., Freese, U., & Niethard, F. U. (1993). The ultrastructure of articular cartilage of the chicken's knee joint. *International Orthopedics*, 17, 113–119.

- Godefroit, P., A. Cau, H. Dong-Yu, F. Escuillié, W. Wenhao, and G. Dyke. 2013. A Jurassic avialan dinosaur from China resolves the early phylogenetic history of birds. *Nature* 498:359–362.
- Godfrey, L., M. Sutherland, D. Boy, and N. Gombert. 1991. Scaling of limb joint surface areas in anthropoid primates and other mammals. *Journal of Zoology* 223:603–625.
- Gunga, H.-C., K. Kirsch, J. Rittweger, L. Röcker, A. Clarke, J. Albertz, A. Wiedemann, S. Mokry, T. Suthau, A. Wehr, W.-D. Heinrich, and H.-P. Schultze. 1999. Body size and body volume distribution in two sauropods from the Upper Jurassic of Tendaguru (Tanzania). *Fossil Record* 2:91–102.
- Gunga, H.-C., T. Suthau, A. Bellmann, A. Friedrich, T. Schwanebeck, S. Stoinski, T. Trippel, K. Kirsch, and O. Hellwich. 2007. Body mass estimations for *Plateosaurus engelhardti* using laser scanning and 3D reconstruction methods. *Naturwissenschaften* 94:623–630. Springer.
- Haines, R. W. 1938. The Primitive Form of Epiphysis in the Long Bones of Tetrapods. *Journal of Anatomy* 72:323–343.
- Haines, R. W. 1941. Epiphysial structure in lizards and marsupials. *Journal of Anatomy* 75:282–294.
- Haines, R. W. 1942. Evolution of epiphyses and of endochondral bone. *Biological reviews of the Cambridge Philosophical Society* 17:267–292. Wiley Online Library.
- Haines, R. W. 1942. The tetrapod knee joint. *Journal of anatomy* 76:270–301.
- Haines, R. W. 1975. The histology of epiphyseal union in mammals. *Journal of Anatomy* 120:1–25.
- Hall, B. K. 2005. *Bones and Cartilage: Developmental and Evolutionary Skeletal Biology*. Academic Press.
- Hay, O. P. 1908. On the habits and the pose of the sauropodous dinosaurs, especially of *Diplodocus*. *The American Naturalist* 42:672–681.
- Holliday, C. M., R. C. Ridgely, J. C. Sedlmayr, and L. M. Witmer. 2010. Cartilaginous epiphyses in extant archosaurs and their implications for reconstructing limb function in dinosaurs. *PLoS One* 5:0013120.
- Hone, D. W. E., A. A. Farke, and M. J. Wedel. 2016. Ontogeny and the fossil record: what, if anything, is an adult dinosaur? *Biology letters* 12:20150947.
- Horner, J. R., K. Padian, and A. de Ricqlès. 2001. Comparative osteohistology of some embryonic and perinatal archosaurs: developmental and behavioral implications for dinosaurs. *Paleobiology* 27:39–58.
- Hotton, N. 1980. An alternative to dinosaur endothermy: the happy wanderers. Pp. 311–350 in E. C. O. Roger D. K. Thomas, ed. *A cold look at the warm-blooded dinosaurs*. Westview Press, Boulder, Colorado.
- Hutchinson, J. R., and V. Allen. 2009. The evolutionary continuum of limb function from early theropods to birds. *Naturwissenschaften* 96:423–448.

Hutchinson, J. R., F. C. Anderson, S. S. Blemker, and S. L. Delp. 2005. Analysis of hindlimb muscle moment arms in *Tyrannosaurus rex* using a three-dimensional musculoskeletal computer model: implications for stance, gait, and speed. *Paleobiology* 31:676–701.

Hutchinson, J. R., V. Ng-Thow-Hing, and F. C. Anderson. 2007. A 3D interactive method for estimating body segmental parameters in animals: application to the turning and running performance of *Tyrannosaurus rex*. *Journal of Theoretical Biology* 246:660–680.

Hutchinson, J. 2001a. The evolution of femoral osteology and soft tissues on the line to extant birds (Neornithes). *Zoological journal of the Linnean Society* 131:169–197.

Hutchinson, J. R. 2001b. The evolution of pelvic osteology and soft tissues on the line to extant birds (Neornithes). *Zoological journal of the Linnean Society* 131:123–168. Oxford University Press.

Hutchinson, J. R. 2006. The evolution of locomotion in archosaurs. *Comptes Rendus Palevo* 5:519–530.

Hutchinson, J. R., K. T. Bates, J. Molnar, V. Allen, and P. J. Makovicky. 2011. A computational analysis of limb and body dimensions in *Tyrannosaurus rex* with implications for locomotion, ontogeny, and growth. *PLoS One* 6, e26037.

Ives, A. R., and T. Garland Jr. 2010. Phylogenetic logistic regression for binary dependent variables. *Systematic Biology* 59:9–26.

Ji, S., Q. Ji, J. Lu, and C. Yuan. 2007. A new giant compsognathid dinosaur with long filamentous integuments from Lower Cretaceous of Northeastern China. *Acta Geol Sin* 81, 8–15.

Kambic, R. E., T. J. Roberts, and S. M. Gatesy. 2014. Long-axis rotation: a missing degree of freedom in avian bipedal locomotion. *Journal of experimental biology* 217:2770–2782.

Kirkland, J. I., D. Burge, and R. Gaston. 1993. A large dromaeosaur (Theropoda) from the Lower Cretaceous of eastern Utah. *Hunteria* 2:1–16.

Lamanna, M. C., H.-D. Sues, E. R. Schachner, and T. R. Lyson. 2014. A new large-bodied oviraptorosaurian theropod dinosaur from the latest Cretaceous of western North America. *PLoS One* 9:e92022.

Langer, M. C., M. D. Ezcurra, O. W. M. Rauhut, M. J. Benton, F. Knoll, B. W. McPhee, F. E. Novas, D. Pol, and S. L. Brusatte. 2017. Untangling the dinosaur family tree. *Nature* 551:E1–E3.

Langer, M. C., and J. Ferigolo. 2013. The Late Triassic dinosauriform *Sacisaurus agudoensis* (Caturrita Formation; Rio Grande do Sul, Brazil): anatomy and affinities. *Geological Society, London, Special Publications* 379:353–392.

Langer, M. C., S. J. Nesbitt, J. S. Bittencourt, and R. B. Irmis. 2013. Non-dinosaurian Dinosauriforma. *Geological Society, London, Special Publications* 379:157–186.

Langer, M. C. 2003. The pelvic and hind limb anatomy of the stem-sauropodomorph *Saturnalia tupiniquim* (Late Triassic, Brazil). *PaleoBios* 23:1–30.

Lee, A. H., and S. Werning. 2008. Sexual maturity in growing dinosaurs does not fit reptilian growth models. *Proc. Natl. Acad. Sci. U. S. A.* 105:582–587.

Lee, Y.-N., R. Barsbold, P. J. Currie, Y. Kobayashi, H.-J. Lee, P. Godefroit, F. Escuillié, and T. Chinzorig. 2014. Resolving the long-standing enigmas of a giant ornithomimosaur *Deinocheirus mirificus*. *Nature* 515:257–260.

Lee, M. S. Y., A. Cau, D. Naish, and G. J. Dyke. 2014. Sustained miniaturization and anatomical innovation in the dinosaurian ancestors of birds. *Science* 345:562–566.

Maidment, S. C. R., K. T. Bates, P. L. Falkingham, C. VanBuren, V. Arbour, and P. M. Barrett. 2014. Locomotion in ornithischian dinosaurs: an assessment using three-dimensional computational modelling. *Biological reviews of the Cambridge Philosophical Society* 89:588–617.

Malda, J., J. C. de Grauw, K. E. M. Benders, M. J. L. Kik, C. H. A. van de Lest, L. B. Creemers, W. J. A. Dhert, and P. R. van Weeren. 2013. Of mice, men and elephants: the relation between articular cartilage thickness and body mass. *PLoS One* 8:e57683..

Mallison, H. 2010. The digital *Plateosaurus* I: body mass, mass distribution, and posture assessed using CAD and CAE on a digitally mounted complete skeleton. *Palaeontol. Electronica* 13:8.

Mallison, H. 2010. The Digital *Plateosaurus* II: An Assessment of the Range of Motion of the Limbs and Vertebral Column and of Previous Reconstructions using a Digital Skeletal Mount. *Acta Palaeontol. Pol.* 55:433–458.

Mallison, H., and O. Wings. 2014. Photogrammetry in paleontology--a practical guide. *Journal of Paleontological Techniques* 12:1–31.

Mao, X., and T. Ryan. 2012. *pgls: Generalized Least Square model for comparative Phylogenetics*. R package version 0.0-1.

Markolf, K. L., and J. M. Morris. 1974. The structural components of the intervertebral disc. A study of their contributions to the ability of the disc to withstand compressive forces. *The Journal of bone and joint surgery* 56:675–687.

Marsh, O. C. 1896. The Dinosaurs of North America. US Geological Survey 16th Annual Report 1894–1895:133–244.

Martinez, R. N., and O. A. Alcober. 2009. A basal sauropodomorph (Dinosauria: Saurischia) from the Ischigualasto Formation (Triassic, Carnian) and the early evolution of Sauropodomorpha. *PLoS One* 4:e4397.

Middleton, K. M., and L. T. English. 2015. Challenges and advances in the study of pterosaur flight. *Canadian journal of zoology* 93:945–959.

Moodie, R. L. 1908. Reptilian epiphyses. *The American journal of anatomy* 7:443–467.

Montes, L., E. de Margerie, J. Castanet, A. de Ricqlès, and J. Cubo. 2005. Relationship between bone growth rate and the thickness of calcified cartilage in the long bones of the Galloanserae (Aves). *Journal of anatomy* 206:445–452.

Müller, R. T., M. C. Langer, S. F. Cabreira, and S. Dias-da-Silva. 2016. The femoral anatomy of *Pampadromaeus barberenai* based on a new specimen from the Upper Triassic of Brazil. *Historical biology* 28:656–665.

Nesbitt, S. J. 2011. The early evolution of archosaurs: Relationships and the origin of major clades. *Bulletin of the American Museum of Natural History* 352:1–292.

Novas, F. E., M. D. Ezcurra, S. Chatterjee, and T. S. Kuttu. 2011. New dinosaur species from the Upper Triassic Upper Maleri and Lower Dharmaram formations of Central India. *Earth and Environmental Science Transactions of the Royal Society of Edinburgh* 101:333–349.

Orme, D., R. Freckleton, G. Thomas, T. Petzoldt, S. Fritz, N. Isaac, and W. Pearse. 2012. Caper: comparative analyses of phylogenetics and evolution in R. R package version 0. 5 2:458. <http://CRAN.R-project.org/package=caper>

Ostrom, J. H. 1978. The osteology of *Compsognathus longipes* Wagner. *Zitteliana* 4, 73–118.

Otero, A. and D. Pol. 2013. Postcranial anatomy and phylogenetic relationships of *Mussaurus patagonicus* (Dinosauria, Sauropodomorpha). *J Vert Paleontol* 33, 1138–1168.

Owen, R. 1841. Report on British fossil reptiles, part II. *Proceedings of the Geological Society of London*. 457:160–204.

Owen, R. 1841. A description of a portion of the skeleton of the *Cetiosaurus*, a gigantic extinct saurian reptile occurring in the oolitic formations of different portions of England. *Proceedings of the Geological Society of London* 457-462

Owen, R. 1875. *Monographs on the British Fossil Reptilia of the Mesozoic Formations: Part II: Genera Bothriospondylus, Cetiosaurus, Omosaurus*. Palaeontological Society Monographs 29:15–93. Palaeontographical Society.

Paradis, E., J. Claude, and K. Strimmer. 2004. APE: Analyses of Phylogenetics and Evolution in R language. *Bioinformatics* 20:289–290.

Paradis, E., and J. Claude. 2002. Analysis of comparative data using generalized estimating equations. *Journal of theoretical biology* 218:175–185.

Peczki, J. 1995 Implications of Body-Mass Estimates for Dinosaurs. *J Vert Paleontol* 14, 520–533.

Perle, A., M. Norell, and J. M. Clark. 1999. A New Maniraptoran Theropod, *Achillobator giganticus* (Dromaeosauridae), from the Upper Cretaceous of Burkhan, Mongolia. *Geology and Mineralogy Chair, National University of Mongolia*.

Phillips, M. J., G. C. Gibb, E. A. Crimp, and D. Penny. 2010. Tinamous and moa flock together: mitochondrial genome sequence analysis reveals independent losses of flight among ratites. *Systematic biology* 59:90–107.

Platt, B. F., S. T. Hasiotis, and D. R. Hiras. 2010. Use of Low-Cost Multistripe Laser Triangulation (MLT) Scanning Technology for Three-Dimensional, Quantitative Paleochronological and Neochronological Studies. *Journal of Sedimentary Research* 80:590–610. GeoScienceWorld.

Rauhut, O. W. M., R. Fechner, K. Remes, and K. Reis. 2011. How to get big in the Mesozoic: the evolution of the sauropodomorph body plan. Pp. 119-149 in N. Klein, K. Remes, C. T. Gee, M. Sander, eds. *Biology of the sauropod dinosaurs: Understanding the life of giants*.

Revell, L. J. 2012. phytools: an R package for phylogenetic comparative biology (and other things). *Methods in ecology and evolution* 3:217–223. Wiley Online Library.

Sander, P. M., N. Klein, E. Buffetaut, G. Cuny, V. Suteethorn, and J. Le Loeuff. 2004. Adaptive radiation in sauropod dinosaurs: bone histology indicates rapid evolution of giant body size through acceleration. *Organisms, diversity & evolution* 4:165–173.

Sander, P. M., A. Christian, M. Clauss, R. Fechner, C. T. Gee, E.-M. Griebeler, H.-C. Gunga, J. Hummel, H. Mallison, S. F. Perry, H. Preuschoft, O. W. M. Rauhut, K. Remes, T. Tütken, O. Wings, and U. Witzel. 2011. Biology of the sauropod dinosaurs: the evolution of gigantism. *Biological reviews of the Cambridge Philosophical Society* 86:117–155.

Schinagl, R. M., D. Gurskis, A. C. Chen, and R. L. Sah. 1997. Depth-dependent confined compression modulus of full-thickness bovine articular cartilage. *Journal of orthopaedic research* 15:499–506.

Schmidt-Nielsen, K., and S.-N. Knut. 1984. *Scaling: Why is Animal Size So Important?* Cambridge University Press, New York.

Seebacher, F. 2001. A new method to calculate allometric length-mass relationships of dinosaurs. *Journal of Vertebrate Paleontology* 21:51–60.

Seeley, H. G. 1888. On the classification of the fossil animals commonly named Dinosauria. *Proceedings of the Royal Society of London* 43:165–171. Royal Society.

Sellers, W. I., L. Margetts, R. A. Coria, and P. L. Manning. 2013. March of the titans: the locomotor capabilities of sauropod dinosaurs. *PloS one*, 8(10).

Sellers, W. I., S. B. Pond, C. A. Brassey, P. L. Manning, and K. T. Bates. 2017. Investigating the running abilities of *Tyrannosaurus rex* using stress-constrained multibody dynamic analysis. *PeerJ* 5:e3420.

Sereno, P. C. 1997. The origin and evolution of Dinosaurs. *Annu Rev Earth Planet Sci* 25, 435–489.

Snover, M. L., and A. G. J. Rhodin. 2007. Comparative ontogenetic and phylogenetic aspects of chelonian chondro-osseous growth and skeletochronology. Pp. 17–39 in J. Wyneken, M. H. Godfrey, V. Bels, ed. *Biology of turtles*. CRC press, Boca Raton, FL.

Stein, K., Z. Csiki, K. C. Rogers, D. B. Weishampel, R. Redelstorff, J. L. Carballido, and P. M. Sander. 2010. Small body size and extreme cortical bone remodeling indicate phyletic dwarfism in *Magyarosaurus dacus* (Sauropoda: Titanosauria). *Proceedings of the National Academy of Sciences of the United States of America* 107:9258–9263.

Stovall, J. W., and W. Langston. 1950. *Acrocanthosaurus atokensis*, a New Genus and Species of Lower Cretaceous Theropoda from Oklahoma. *American Midland Naturalist* 43:696–728.

- Sues Hans-Dieter, Nesbitt Sterling J., Berman David S, and Henrici Amy C. 2011. A late-surviving basal theropod dinosaur from the latest Triassic of North America. *Proceedings of the Royal Society B: Biological Sciences* 278:3459–3464.
- Therrien, F., and D. M. Henderson. 2007. My theropod is bigger than yours ... or not: estimating body size from skull length in theropods. *Journal of Vertebrate Paleontology* 27:108–115.
- Thorp, B. H. 1988. Relationship between the rate of longitudinal bone growth and physeal thickness in the growing fowl. *Res. Vet. Sci.* 45:83–85.
- Tsai, H.P. 2015. Archosaur hip joint anatomy and its significance in body size and locomotor evolution. (Doctoral dissertation, University of Missouri, Columbia). doi: <https://hdl.handle.net/10355/50154>.
- Tsai, H. P., and C. M. Holliday. 2015. Articular soft tissue anatomy of the archosaur hip joint: Structural homology and functional implications. *Journal of Morphology* 276:601–630.
- Tsai, H. P., K. M. Middleton, J. R. Hutchinson, and C. M. Holliday. 2018. Hip joint articular soft tissues of non-dinosaurian Dinosauromorpha and early Dinosauria: evolutionary and biomechanical implications for Saurischia. *Journal of Vertebrate Paleontology* 38:e1427593.
- Tsai, H. P., M. L. Turner, A. R. Manafzadeh, and S. M. Gatesy. 2019. Contrast-enhanced XROMM reveals in vivo soft tissue interactions in the hip of *Alligator mississippiensis*. *Journal of Anatomy* 236: 288-304.
- Tschopp, E., O. Mateus, and R. B. J. Benson. 2015. A specimen-level phylogenetic analysis and taxonomic revision of Diplodocidae (Dinosauria, Sauropoda). *PeerJ* 3:e857. peerj.com.
- Turner, A. H., P. J. Makovicky, and M. A. Norell. 2012. A Review of Dromaeosaurid Systematics and Paravian Phylogeny. *Bulletin of the American Museum of Natural History* 371:1–206.
- Turner, A. H., and S. J. Nesbitt. 2013. Body size evolution during the Triassic archosauriform radiation. *Geological Society, London, Special Publications* 379:573–597.
- Turner, A. H., D. Pol, J. A. Clarke, G. M. Erickson, and M. A. Norell. 2007. A basal dromaeosaurid and size evolution preceding avian flight. *Science* 317:1378–1381.
- Wilson, J. A., and P. C. Sereno. 1998. Early Evolution and Higher-Level Phylogeny of Sauropod Dinosaurs. *Society of Vertebrate Paleontology Memoir* 5:1–68.
- Wilson, J. A., and M. T. Carrano. 1999. Titanosaurs and the origin of “wide-gauge” trackways: a biomechanical and systematic perspective on sauropod locomotion. *Paleobiology* 25:252–267.
- Wilson, J. A. 2005. Overview of sauropod phylogeny and evolution. Pp. 15–49 in K. C. Rogers and J. Wilson, eds. *The Sauropods: Evolution and Paleobiology*. University of California Press, Berkeley, CA.
- Xu, X., Q. Ma, and D. Hu. 2010. Pre-*Archaeopteryx* coelurosaurian dinosaurs and their implications for understanding avian origins. *Chinese Science Bulletin* 55:3971–3977.

Xu, X., Q. Tan, J. Wang, X. Zhao, and L. Tan. 2007. A gigantic bird-like dinosaur from the Late Cretaceous of China. *Nature* 447:844–847.

Xu, X., H. You, K. Du, and F. Han. 2011. An *Archaeopteryx*-like theropod from China and the origin of Avialae. *Nature* 475:465–470.

Yates, A. M., M. F. Bonnan, J. Neveling, A. Chinsamy, and M. G. Blackbeard. 2010. A new transitional sauropodomorph dinosaur from the Early Jurassic of South Africa and the evolution of sauropod feeding and quadrupedalism. *Proceedings of the Royal Society B: Biological Sciences* 277:787–794.

Yates, A. M., and J. W. Kitching. 2003. The earliest known sauropod dinosaur and the first steps towards sauropod locomotion. *Proceedings of the Royal Society of London. Series B: Biological Sciences* 270:1753–1758.

Yates, A. M. 2004. *Anchisaurus polyzelus* (Hitchcock): the smallest known Sauropod Dinosaur and the evolution of gigantism among Sauropodomorph Dinosaurs. *Postilla* 230:1-58.

Zhao, X., R. B. J. Benson, S. L. Brusatte, and P. J. Currie. 2010 The postcranial skeleton of *Monolophosaurus jiangi* (Dinosauria: Theropoda) from the Middle Jurassic of Xinjiang, China, and a review of Middle Jurassic Chinese theropods. *Geol Mag* 147, 13–27.

*The phylogenetic trees and character matrices used in this study are electronically archived on Dryad (doi:10.5061/dryad.hmgqnk9dc)

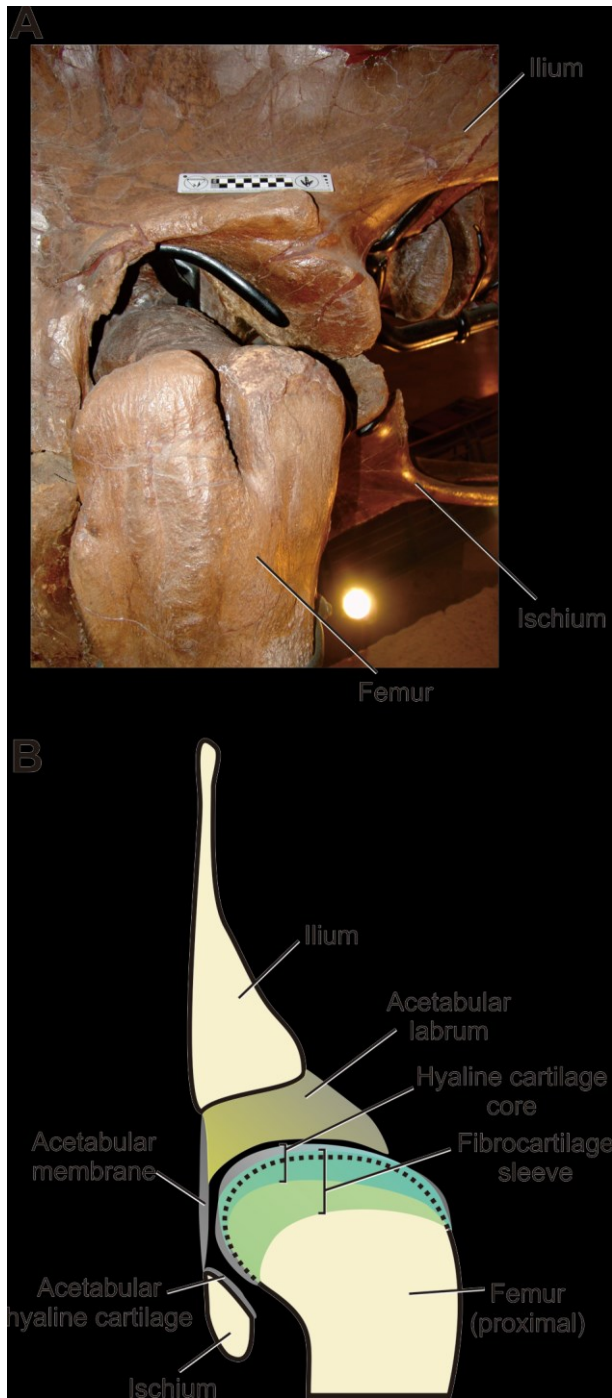
Figure legends

Figure 1. **A.** Articulated left hip joint of *Tyrannosaurus* (FMNH PR 2081) in laterosuperior oblique view. **B.** Generalized anatomical diagram of archosaurian hip joint soft tissue articulation. The hip joint is shown in caudal view, with the pelvis in transverse section.

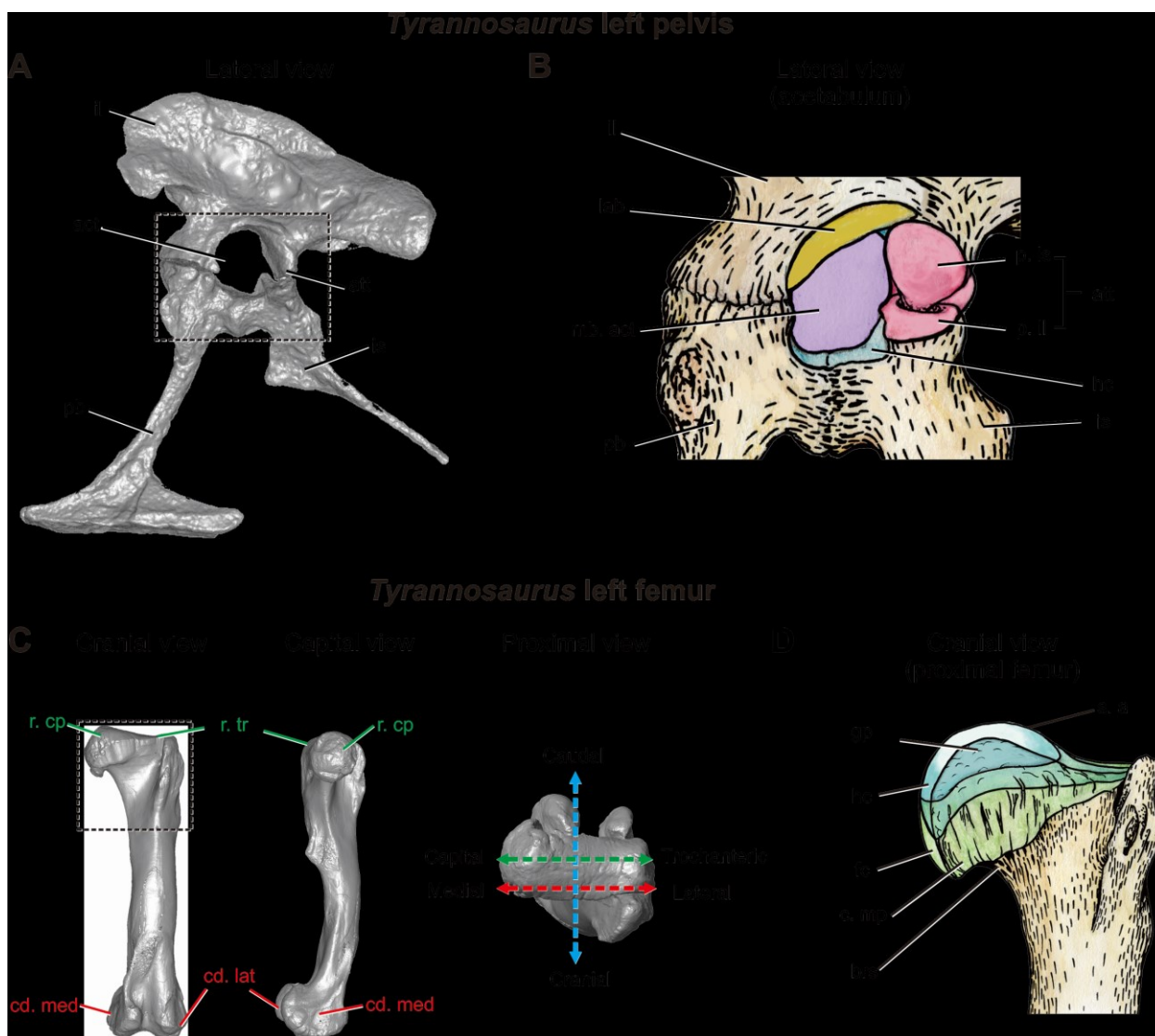


Figure 2. **A.** 3D surface model of *Tyrannosaurus* left hemipelvis (FMNH PR 2081) in lateral view. **B.** Schematic representation of acetabular soft tissues (black dotted inset in A), excluding joint ligaments. **C.** 3D surface model of the associated *Tyrannosaurus* left femur in cranial, medial, and proximal views. Relative orientation between the femoral head-greater trochanter axis (green labels) and the mediolateral axis of the distal condyles (red labels) determines the orthogonal reference planes used to describe anatomical structures, shown as dotted lines in proximal views of each femur. The cranio-trochanteric plane is represented in green, mediolateral plane in red, craniocaudal plane in blue. **D.** Schematic representation of proximal femoral soft tissues (black dotted inset in C), excluding joint ligaments. Tissues' nomenclature and color schemes are labeled according to homology inferences in Tsai and Holliday (2014).

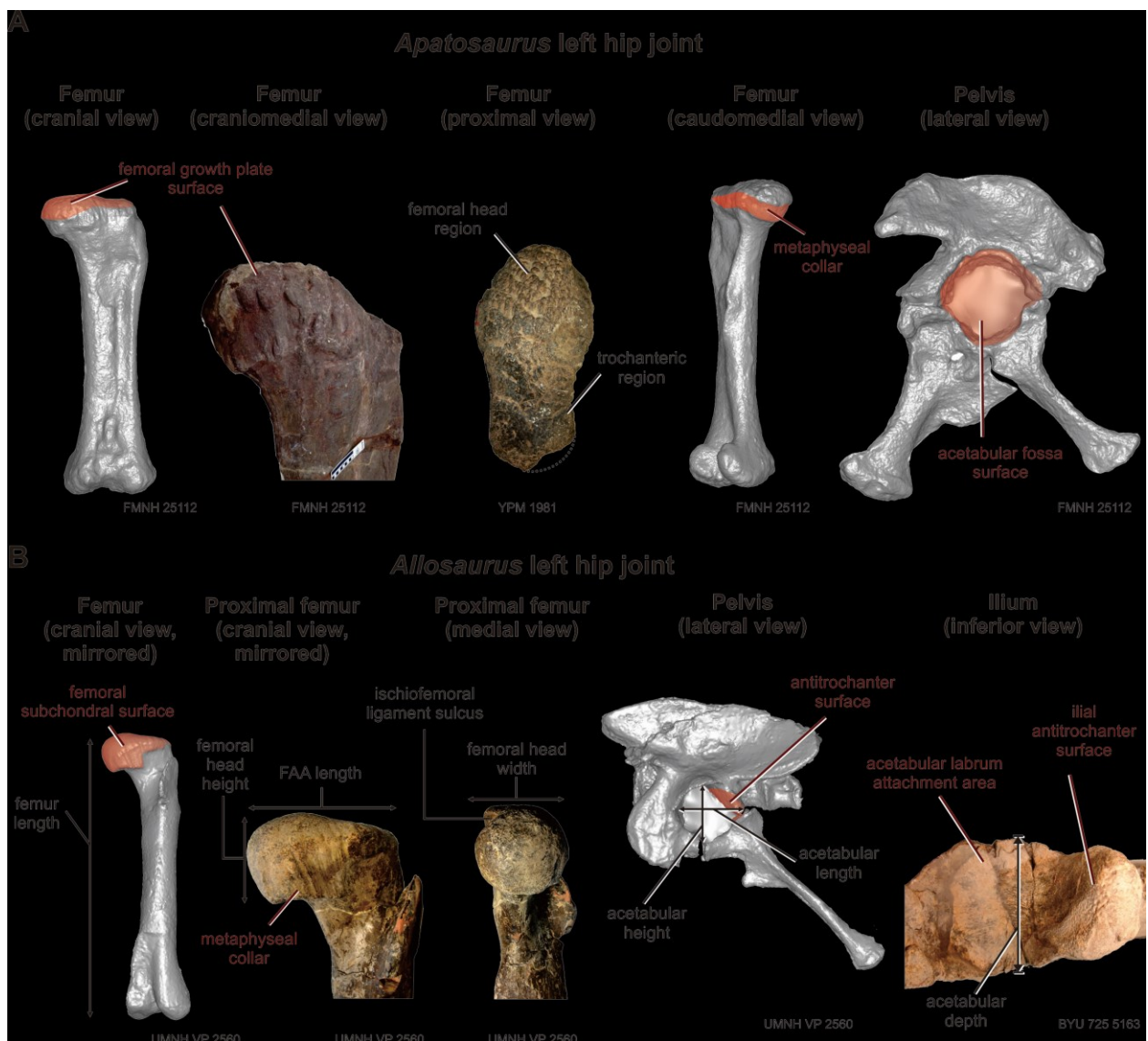


Figure 3. Discrete osteological correlates and continuous hip joint metrics were taken from the hip joints of saurischians. **A.** Femoral and pelvic elements of *Apatosaurus*. **B.** Femoral and pelvic elements of *Allosaurus*. Surface areas of soft tissue attachments (red) were measured from 3D models.

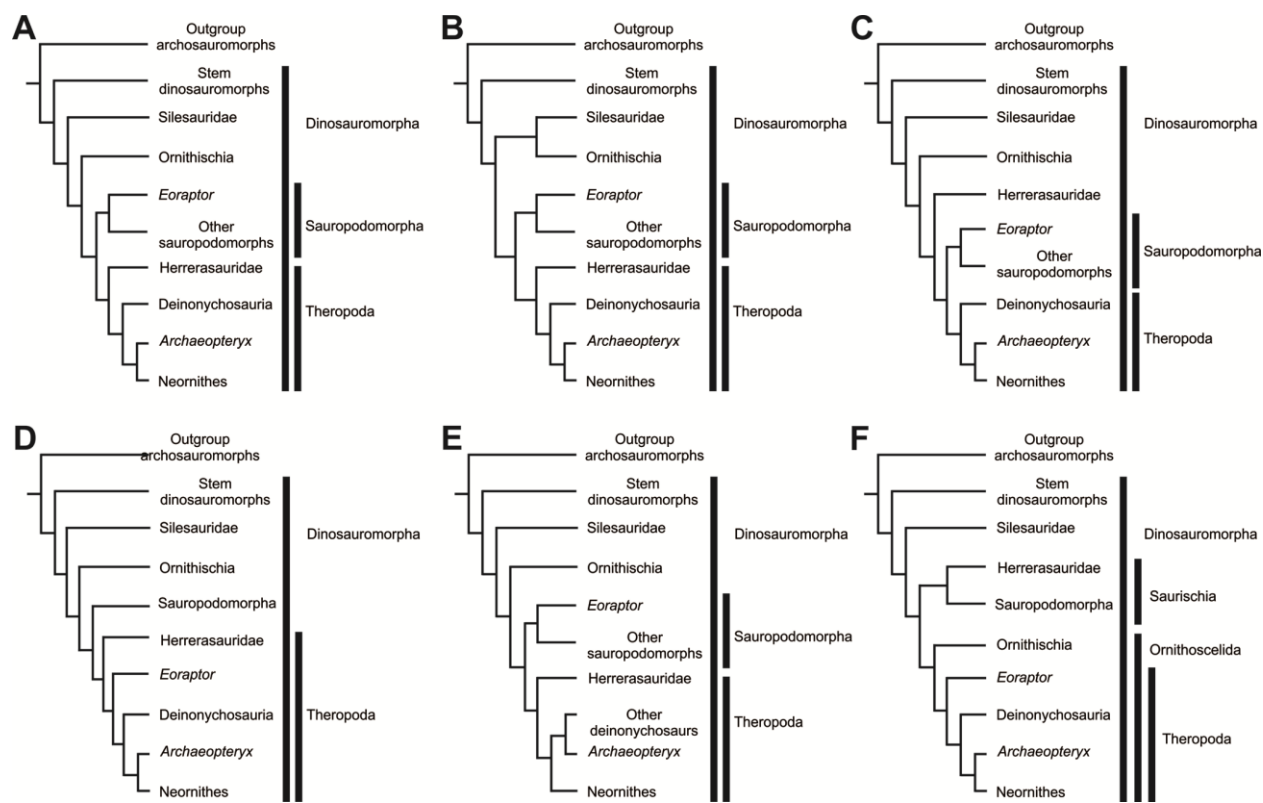


Figure 4. Simplified topologies of phylogenetic trees used in this study. **A.** The “consensus” phylogenetic tree based on published studies. **B.** Alternate placement of Silesauridae as stem ornithischians. **C.** Alternate placement of Herrerasauridae as the sister taxon to Theropoda + Sauropodomorpha. **D.** Alternate placement of *Eoraptor* as a basal theropod, rather than as a basal sauropodomorph. **E.** Alternate placement of *Archaeopteryx* as a stem-deinonychosaur, rather than as the basal-most avialan. **F.** Alternative tree topology of Dinosauria as proposed by Baron et al., 2017.

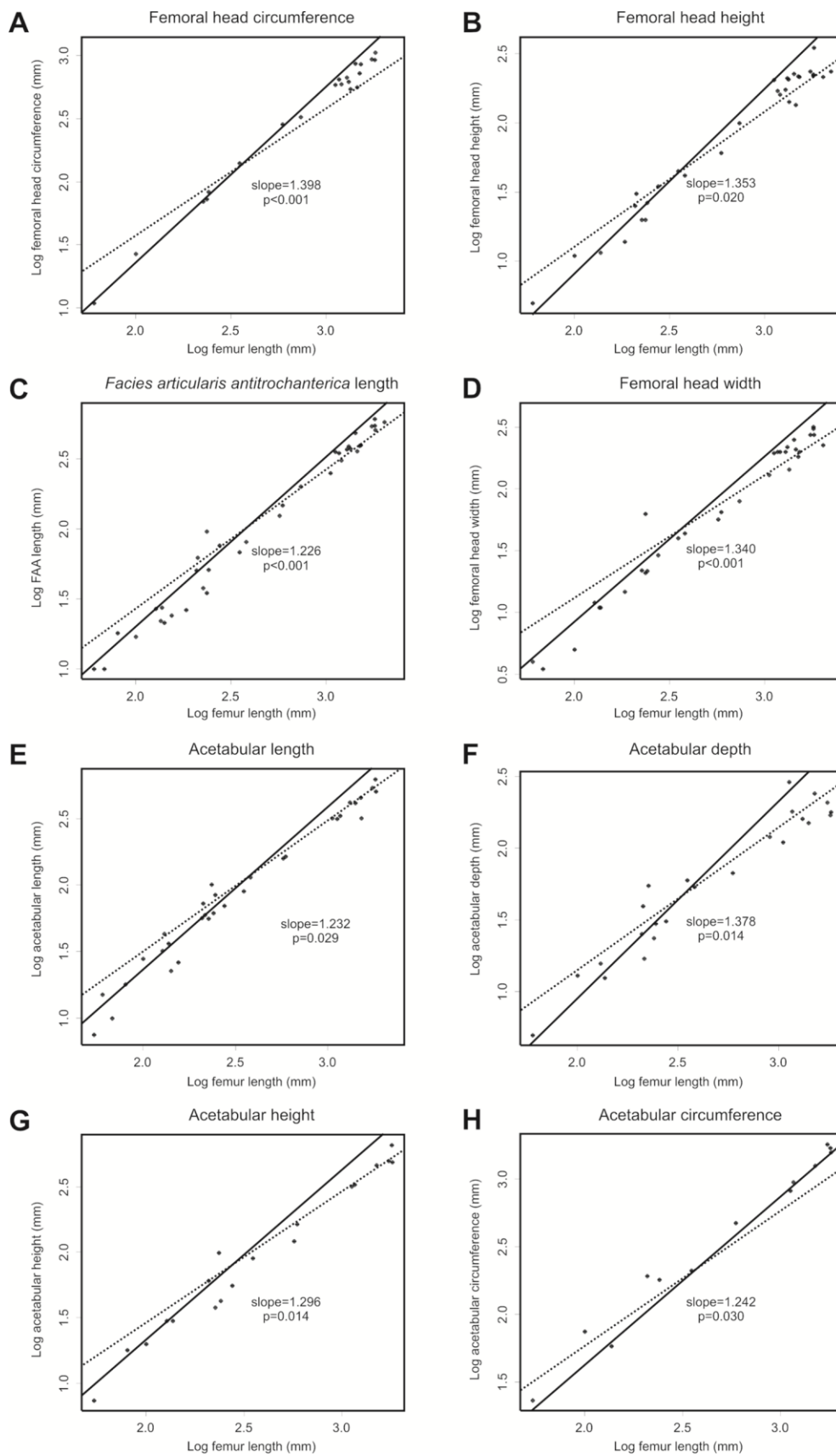


Figure 5. Phylogenetic generalized reduced major axis regressions of hip joint linear dimensions vs. log femur length in the sauropod lineage using the “consensus” tree. Null hypothesized slopes ($= 1$) is signified by the black dotted line. **A.** Femoral head circumference. **B.** Femoral head height. **C.** *Facies articularis antitrochanterica* length. **D.** Femoral head width. **E.** Acetabular length. **F.** Acetabular depth. **G.** Acetabular height. **H.** Acetabular circumference. All hip joint linear dimensions scale to positive allometry relative to femur length. Note that relative linear dimensions of the subchondral (bony) femoral and acetabular surfaces remained consistent across the body size spectrum in the sauropod lineage.

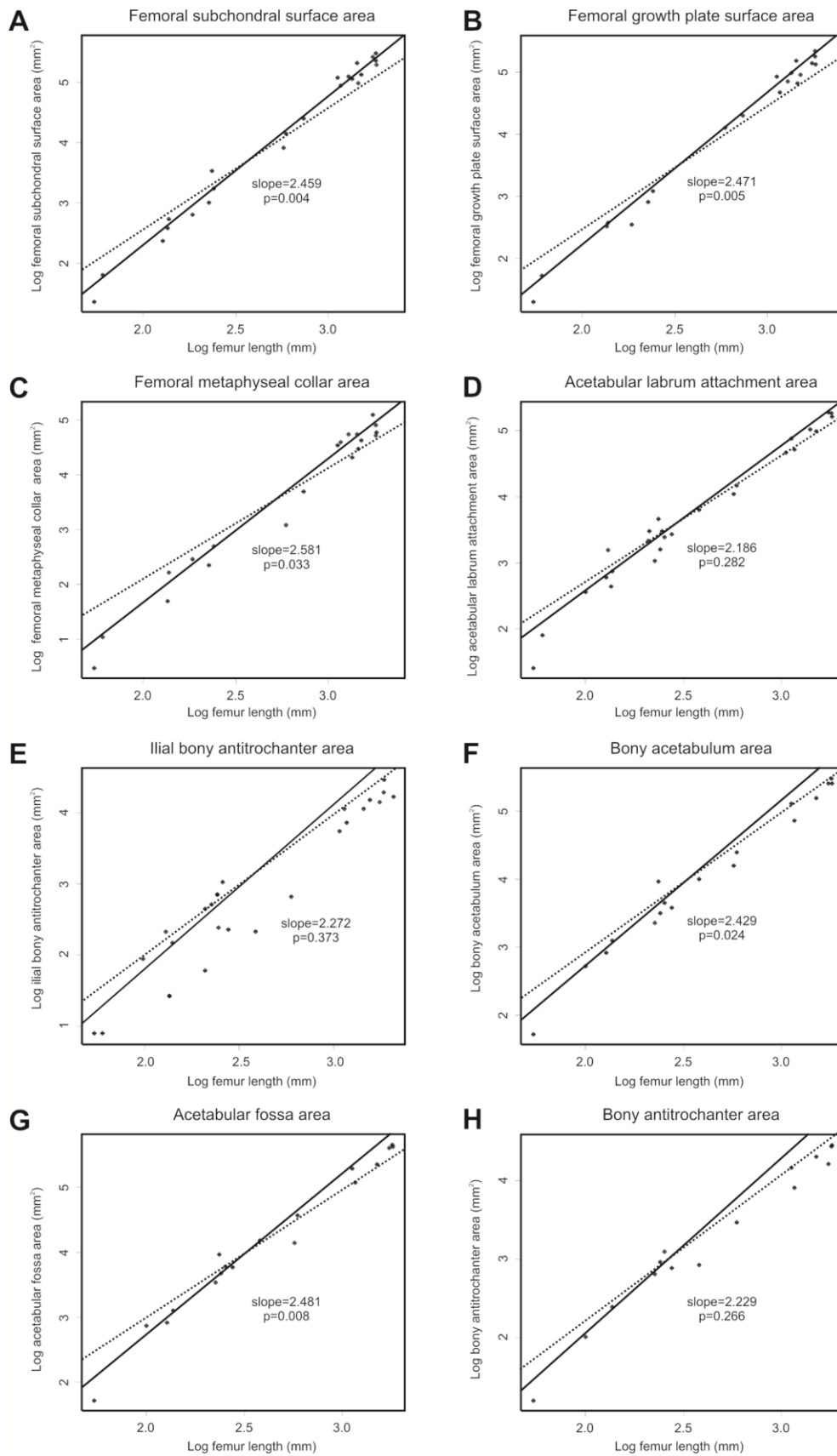


Figure 6. Phylogenetic generalized reduced major axis regressions of hip joint surface area dimensions vs. log femur length in the sauropod lineage using the “consensus” tree. Null hypothesized slopes ($= 2$) is signified by the black dotted line. **A.** Femoral subchondral surface area. **B.** Femoral growth plate area. **C.** Femoral metaphyseal collar area. **D.** Acetabular labrum attachment surface area. **E.** Iliac bony antitrochanter area. **F.** Bony acetabulum area. **G.** Acetabular fossa area. **H.** Bony antitrochanter area. Most hip joint surface area dimensions scale to positive allometry relative to femur length. Attachment areas for acetabular labrum, the iliac portion of the antitrochanter, and the whole antitrochanter scale to isometry relative to femur length. Note that relative surface area dimensions of the subchondral (bony) femoral and acetabular surfaces remained consistent across the body size spectrum in the sauropod lineage.

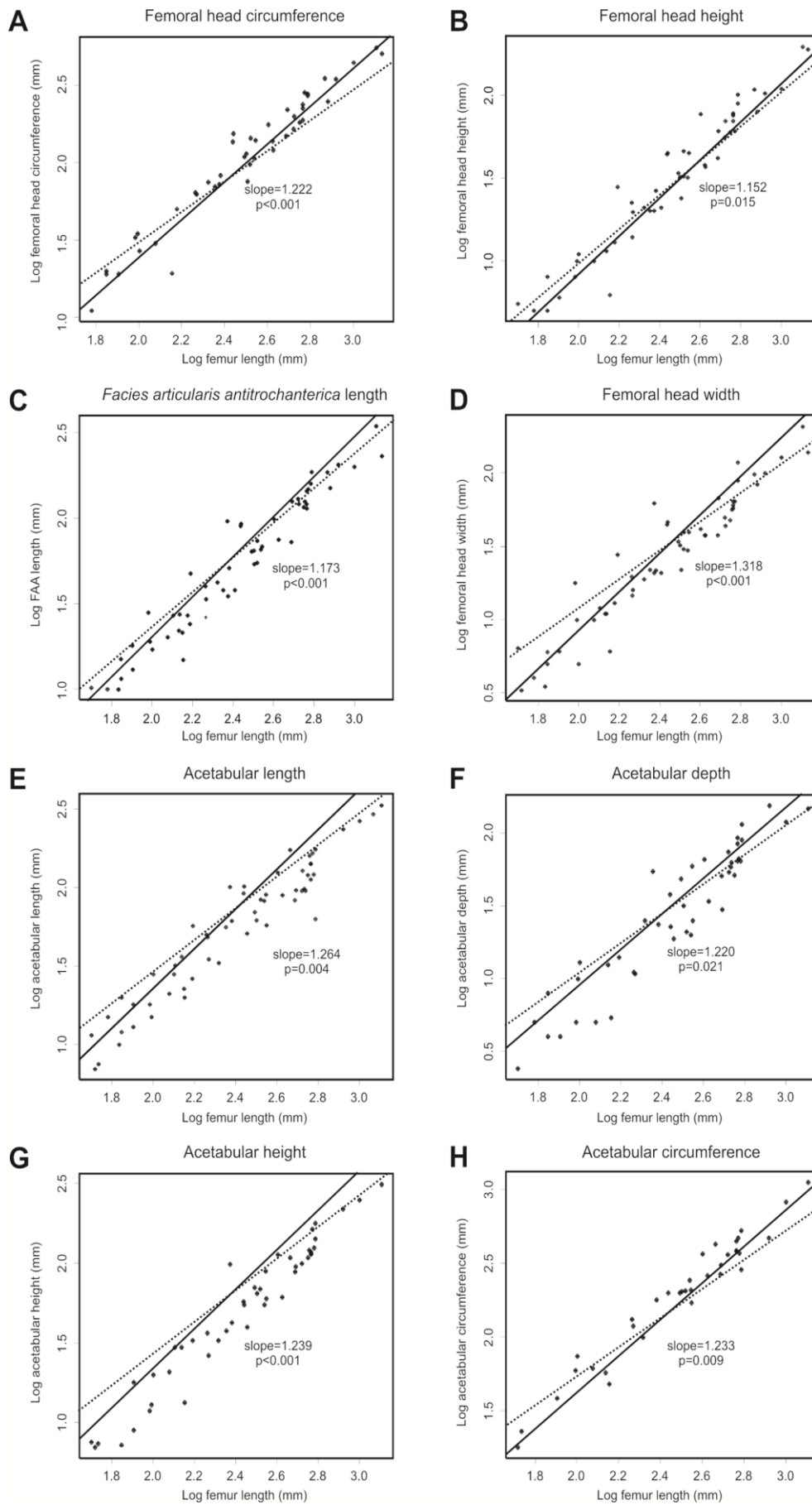


Figure 7. Phylogenetic generalized reduced major axis regressions of hip joint linear dimensions vs. log femur length in the theropod lineage using the “consensus” tree. Null hypothesized slopes ($= 1$) is signified by the black dotted line. **A.** Femoral head circumference. **B.** Femoral head height. **C.** *Facies articularis antitrochanterica* length. **D.** Femoral head width. **E.** Acetabular length. **F.** Acetabular depth. **G.** Acetabular height. **H.** Acetabular circumference. All hip joint linear dimensions scale to positive allometry relative to femur length. Note that relative linear dimensions of the subchondral (bony) femoral and acetabular surfaces remained consistent across the body size spectrum in the theropod lineage.

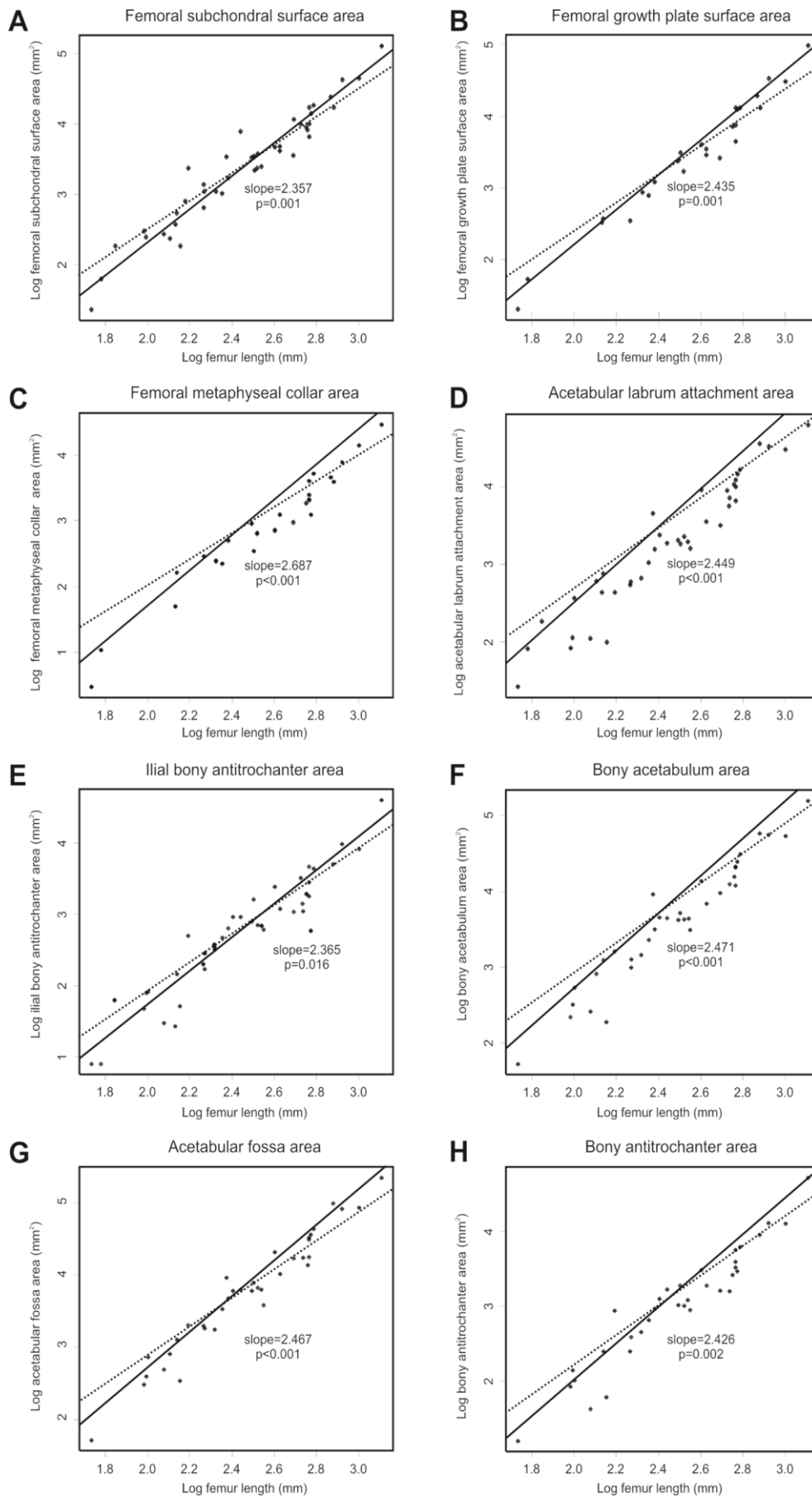


Figure 8. Phylogenetic generalized reduced major axis regressions of hip joint surface area dimensions vs. log femur length in the theropod lineage using the “consensus” tree. Null hypothesized slopes ($= 2$) is signified by the black dotted line. **A.** Femoral subchondral surface area. **B.** Femoral growth plate area. **C.** Femoral metaphyseal collar area. **D.** Acetabular labrum attachment surface area. **E.** Iliac bony antitrochanter area. **F.** Bony acetabulum area. **G.** Acetabular fossa area. **H.** Bony antitrochanter area. All hip joint surface area dimensions scale to positive allometry relative to femur length. Note that relative surface area dimensions of the subchondral (bony) femoral and acetabular surfaces remained consistent across the body size spectrum in the theropod lineage.

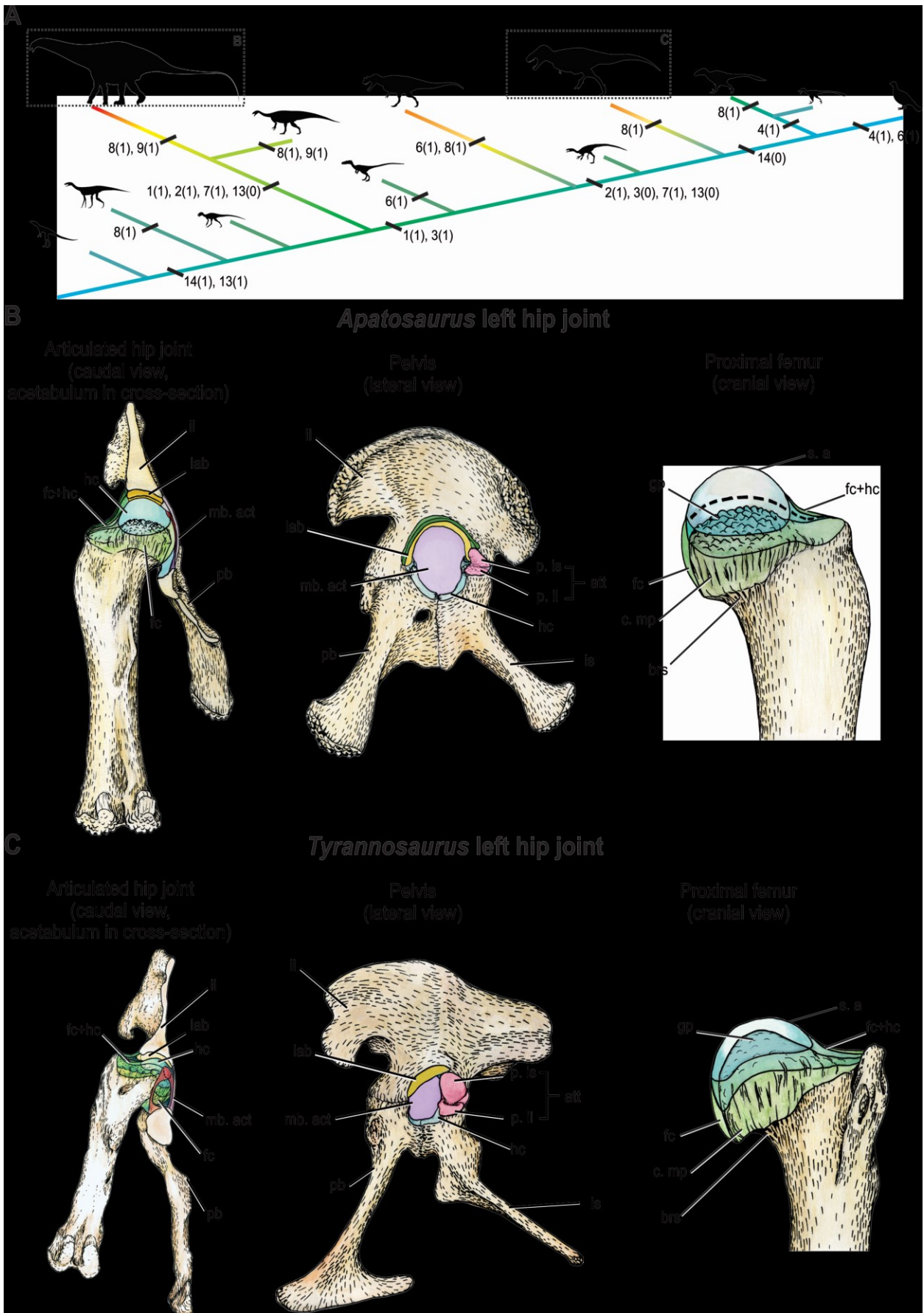


Figure 9. Body size evolution and hip joint soft tissue reconstructions of representative gigantic saurischians. **A.** Simplified phylogenetic tree showing major evolutionary transitions in body size and hip joint anatomy. Ancestral character states were estimated using maximum likelihood. Branches are color coded in reference to body size, with warmer colored branches denoting larger body size. Character gains are marked by numerical designations summarized in Table 5. Character gains are indicated by ones; losses are indicated by zeros. Silhouettes of taxa (phylogics) depicted here are provided by S. Hartman, T. M. Keesey, N. Kelley, A. A. Farke, B. McFeeters, S. Werning, E. Willoughby, and E. Östman (Wikipedia user) under Creative Commons licensing. **B.** The hip joint of *Apatosaurus* articulated with thick layers of femoral epiphyseal cartilage, with limited contribution of supraacetabular soft tissues. Minimal estimate of femoral hyaline cartilage thickness (based on CCF of juvenile *Struthio*) is shown as the dotted line. **C.** Hip joint articulation in *Tyrannosaurus* required extensive amounts of supraacetabular articular pads (labrum and menisci), as well as contact between the femoral neck and the antitrochanter. Tissues are labeled and color-coded based on inferred homology described in Tsai and Holliday (2014). *Tyrannosaurus* hip joint cross section based on Bates and Schachner, 2011. See Table 1 for anatomical abbreviations.

TABLES

Table 1. Anatomical abbreviations.

att	antitrochanter	l. ilf	iliofemoral ligament
brs	bursa	l. isf	ischiofemoral ligament
cc	calcified cartilage	l. pf	pubofemoral ligament
cd. med	medial condyle		
cd. lat	lateral condyle	m. istr	<i>m. ischiotrochantericus</i>
c. mp	metaphyseal collar	mb. act	acetabular membrane
cn	cartilage cone	pb	pubis
fm	femur	ppi	pubic peduncle of ilium
fov	fovea capitis	pcf	peripheral collagen fiber
fc	fibrocartilage	pd. pb	pubic peduncle of ilium
gp	growth plate	pd. is	ischial peduncle of ilium
hc	hyaline cartilage		
hcc. att	Antitrochanter hyaline cartilage core	r. cp	capital region
il	ilium	r. tr	trochanteric region
is	ischium	s. a	articular surface
lab	acetabular labrum	sc. isf	ischiofemoral ligament sulcus
l. cf	ligamentum capitis femoris	tr. cn	cartilage cone trough

Table 2. Osteological correlates of hip joint soft tissues.

Soft tissue structure	Osteological correlates
Iliofemoral ligament: Origin	Craniodorsal acetabular rim (pubic peduncle of ilium).
Iliofemoral ligament: Insertion	Craniolateral metaphyseal collar of the proximal femur.
Acetabular labrum	Ventral side of supraacetabular rim (cranial portion of acetabular roof).
Acetabular membrane	Unossified inner acetabular wall (the inner acetabular foramen).
Antitrochanter fibrocartilage	Laterally oriented surface of the bony antitrochanter; surface of antitrochanter hyaline cartilage core.
Antitrochanter hyaline cartilage core	Growth plate surfaces of the ilio- and ischial peduncles (archosaur).
Pubofemoral ligament: Origin	Cranioventral (pubic) rim of the inner acetabular foramen.
Ischiofemoral ligament: Origin	Caudoventral (ischial) rim of the inner acetabular foramen.
Ischiofemoral ligament: Passage	Ischiofemoral ligament sulcus on the proximal femoral metaphysis.
Ligamentum capitis femoris: Insertion (confluence of pubofemoral and ischiofemoral ligaments)	Cranial surface of the posteromedial tuber (plesiomorphic); flat or concave surfaces on the femoral head (Aves and some coelurosaurs).
Expanded metaphyseal attachment for fibrocartilage sleeve	Striated, elevated cortical bone surface on the metaphysis.
Hyaline cartilage core	Calcified cartilage-covered growth plate overlying subchondral trabecular bone.
Thick layer of hyaline cartilage	Irregularly rugose growth plate surface.
Extension of the cartilage cone into the metaphyseal growth plate	Longitudinal groove on the proximal femoral growth plate surface.
Synovial bursa	Exposed patch of metaphyseal trabecular bone surrounded by cortical bone.

Table 3. Results of phylogenetic logistic regressions between body size (femur length) and hip joint osteological characters in the sauropod lineage using the “consensus” phylogenetic tree. Significant associations between body size and the derived character state are noted by an asterisk (*). Lack of significant correlation is denoted as “NS”. Characters which transitions cannot be predicted by femur length using phylogenetic logistic regression are indicated by “N/A”. Invariable characters are not analyzed. Only the presence of rugose surface texture on the proximal femoral growth plate is positively correlated with body size.

Character#	Character name	Character states	P-value	Direction of relationship
1	Perforated acetabulum	(0) absent (1) present	0.163	NS
2	Lateral expansion of the supraacetabular rim	(0) expanded (1) reduced	0.228	NS
3	Orientation of the supraacetabular rim	(0) laterally oriented (1) ventrolaterally oriented	0.391	NS
4	Expansion of the bony antitrochanter	(0) unexpanded (1) expanded	Not analyzed	
5	Shape of the ischial peduncle of the ilium	(0) flat (1) cranially concave	N/A	
6	Co-ossification of the bony antitrochanter	(0) open synchondrosis (1) co-ossified	Not analyzed	
7	Femoral head deflection	(0) craniomedially deflected (1) medially deflected	0.410	NS
8	Surface texture of the proximal femoral growth plate	(0) smooth (1) rugose	0.003*	Positively correlated
9	Capital concentration of irregular rugosities on the femoral head	(0) absent (1) present	N/A	
10	Transphyseal striations	(0) absent (1) present	0.139	NS
11	Fovea capitis	(0) indistinct (1) distinct (planar or concave)	Not analyzed	

12	Ischiofemoral ligament sulcus	(0) shallow (1) deep	0.671	NS
13	Cartilage cone trough	(0) absent (1) distinct	0.116	NS
14	Expanded metaphyseal Collar	(0) Unexpanded (1) Expanded	0.667	NS

Table 4. Results of phylogenetic logistic regressions between body size (femur length) and hip joint osteological characters in the theropod lineage using the “consensus” phylogenetic tree. Significant associations between body size and the derived character state are noted by an asterisk (*). Lack of significant correlation is denoted as “NS”. Characters which transitions cannot be predicted by femur length using phylogenetic logistic regression are indicated by “N/A”. Invariable characters are not analyzed. No discrete character showed association with body size.

Character#	Character name	Character states	P-value	Probability of derived character state
1	Perforated acetabulum	(0) absent (1) present	0.762	NS
2	Lateral expansion of the supraacetabular rim	(0) expanded (1) reduced	0.880	NS
3	Orientation of the supraacetabular rim	(0) laterally oriented (1) ventrolaterally oriented	0.176	NS
4	Expansion of the bony antitrochanter	(0) unexpanded (1) expanded	0.794	NS
5	Shape of the ischial peduncle of the ilium	(0) flat (1) cranially concave	Not analyzed	
6	Co-ossification of the bony antitrochanter	(0) open synchondrosis (1) co-ossified	0.992	NS
7	Femoral head deflection	(0) craniomedially deflected (1) medially deflected	0.895	NS
8	Surface texture of the proximal femoral growth plate	(0) smooth (1) rugose	N/A	
9	Concentration of irregular rugosities on the femoral head	(0) absent (1) present	0.586	NS
10	Transphyseal striations	(0) absent (1) present	0.206	NS
11	Fovea capitis	(0) indistinct (1) distinct (planar or	0.687	NS

		concave)		
12	Ischiofemoral ligament sulcus	(0) shallow (1) deep	N/A	
13	Cartilage cone trough	(0) absent (1) distinct	0.921	NS
14	Expanded metaphyseal Collar	(0) Unexpanded (1) Expanded	0.320	NS

Table 5. P-values of phylogenetic logistic regressions between body size (femur length) and hip joint osteological characters in the sauropod lineage using alternative tree topologies. Significant associations between body size and the derived character state are noted by an asterisk (*). Characters which transitions cannot be predicted by femur length using phylogenetic logistic regression are indicated by “N/A”. Invariable characters are not analyzed.

Character	Silesauridae as stem ornithischians	Herrerasauridae as stem saurischians	<i>Eoraptor</i> as stem theropod	<i>Archaeopteryx</i> as stem deinonychosaur	Baron, et al., (2017) tree topology
Perforated acetabulum	0.160	0.146	0.151	0.163	0.150
Lateral expansion of the supraacetabular rim	0.228	0.230	0.227	0.228	0.234
Orientation of the supraacetabular rim	0.390	0.416	0.375	0.392	0.380
Expansion of the bony antitrochanter	Not Analyzed				
Shape of the ischial peduncle of the ilium	N/A	N/A	N/A	N/A	N/A
Co-ossification of the bony antitrochanter	Not Analyzed				
Femoral head deflection	0.403	0.413	0.541	0.410	0.571
Surface texture of the proximal femoral growth plate	0.003	0.003	0.007	0.003	0.008
Concentration of irregular rugosities on the femoral head	N/A	N/A	N/A	N/A	N/A
Transphyseal striations	0.139	0.138	0.139	0.139	0.139
Fovea capitis	Not Analyzed				

Ischiofemoral ligament sulcus	0.671	0.6534552	0.673274 7	0.6709719	0.632
Cartilage cone trough	0.121	0.118	0.116	0.116	0.118
Expanded metaphyseal Collar	0.657	0.660	0.667	0.667	0.668

Table 6. P-values of phylogenetic logistic regressions between body size (femur length) and hip joint osteological characters in the theropod lineage using alternative tree topologies. Significant patterns in correlations are noted by an asterisk (*). Characters which transitions cannot be predicted by femur length using phylogenetic logistic regression are indicated by “N/A”. Invariable characters are not analyzed.

Character	Silesauridae as stem ornithischians	Herrerasauridae as stem saurischians	<i>Eoraptor</i> as stem theropod	<i>Archaeopteryx</i> as stem deinonychosaur	Baron, et al., (2017) tree topology
Perforated acetabulum	0.763	0.751	0.803	0.766	0.805
Lateral expansion of the supraacetabular rim	0.881	0.886	0.947	0.945	0.952
Orientation of the supraacetabular rim	0.173	0.191	0.185	0.179	0.185
Expansion of the bony antitrochanter	0.793	0.792	0.795	0.914	0.794
Shape of the ischial peduncle of the ilium	Not analyzed				
Co-ossification of the bony antitrochanter	0.989	0.999	0.993	N/A	0.993
Femoral head deflection	0.896	0.893	0.850	0.901	0.840
Surface texture of the proximal femoral growth plate	N/A	N/A	N/A	N/A	N/A
Concentration of irregular rugosities on the femoral head	0.586	0.584	0.638	0.588	0.641
Transphyseal striations	0.206	0.204	0.206	0.213	0.209
Fovea capitis	0.688	0.689	0.688	0.688	0.692

Ischiofemoral ligament sulcus	N/A	N/A	N/A	N/A	N/A
Cartilage cone trough	0.917	0.925	0.921	0.926	0.923
Expanded metaphyseal Collar	0.317	0.319	0.320	0.331	0.321

Table 7. Reduced major axis regressions between body size (femur length) and hip joint measurements in the sauropod lineage using the “consensus” tree (Fig. 3a). 95% CI = 95% confidence intervals (upper and lower). “Null slope” = isometric scaling.

Character	Allometry	Null slope	RMA slope	R ²	P-value (diff. from isometry)	95% CI	
Femoral head circumference	Positive	1	1.398	0.947	<0.001	1.249	1.547
Femoral head height	Positive	1	1.353	0.575	0.020	1.015	1.692
<i>Facies articularis antitrochanterica</i> length	Positive	1	1.226	0.910	<0.001	1.104	1.348
Femoral head width	Positive	1	1.340	0.808	<0.001	1.129	1.550
Acetabular length	Positive	1	1.232	0.750	0.029	1.004	1.461
Acetabular depth	Positive	1	1.378	0.682	0.014	1.038	1.718
Acetabular height	Positive	1	1.296	0.902	0.004	1.090	2.502
Acetabular circumference	Positive	1	1.242	0.913	0.030	1.005	1.478
Femoral subchondral surface area	Positive	2	2.459	0.916	0.004	2.137	2.782
Femoral growth plate surface area	Positive	2	2.471	0.922	0.005	2.131	2.811
Femoral metaphyseal collar surface area	Positive	2	2.581	0.777	0.033	1.985	3.176
Acetabular labrum attachment surface area	Isometry	2	2.186	0.839	0.282	1.819	2.553
Iliac bony antitrochanter area	Isometry	2	2.272	0.553	0.373	1.609	2.934
Bony acetabulum	Positive	2	2.429	0.902	0.024	2.030	2.829
Acetabular fossa	Positive	2	2.481	0.919	0.008	2.110	2.851

Bony antitrochanter surface area	Isometry	2	2.229	0.880	0.266	1.774	2.684
----------------------------------	----------	---	-------	-------	-------	-------	-------

Table 8. Reduced major axis regressions between body size (femur length) and hip joint measurements in the theropod lineage using the “consensus” tree (Fig. 3a). 95% CI = 95% confidence intervals (upper and lower). “Null slope” = isometric scaling.

Character	Allometry	Null slope	RMA slope	R ²	P-value (diff. from isometry)	95% CI	
Femoral head circumference	Positive	1	1.222	0.947	<0.001	1.137	1.308
Femoral head height	Positive	1	1.152	0.849	0.015	1.023	1.282
<i>Facies articularis antitrochanterica</i> length	Positive	1	1.173	0.936	<0.001	1.094	1.253
Femoral head width	Positive	1	1.318	0.929	<0.001	1.222	1.413
Acetabular length	Positive	1	1.264	0.659	0.004	1.067	1.461
Acetabular depth	Positive	1	1.220	0.704	0.021	1.017	1.423
Acetabular height	Positive	1	1.239	0.905	<0.001	1.124	1.353
Acetabular circumference	Positive	1	1.233	0.812	0.009	1.044	1.158
Femoral subchondral surface area	Positive	2	2.357	0.912	0.001	2.139	2.575
Femoral growth plate surface area	Positive	2	2.435	0.938	0.001	2.181	2.688
Femoral metaphyseal collar surface area	Positive	2	2.687	0.889	<0.001	2.312	3.062
Acetabular labrum attachment surface area	Positive	2	2.449	0.908	<0.001	2.208	2.689
Iliac bony antitrochanter area	Positive	2	2.365	0.836	0.016	2.047	2.683
Bony acetabulum	Positive	2	2.471	0.919	<0.001	2.226	2.715
Acetabular fossa	Positive	2	2.467	0.921	<0.001	2.226	2.707

Bony antitrochanter surface area	Positive	2	2.426	0.899	0.002	2.148	2.703
----------------------------------	----------	---	-------	-------	-------	-------	-------